

NASA/CR—1999-208686



Unsteady Diffusion Flames: Ignition, Travel, and Burnout (SUBCORE Project: Simplified *Unsteady Burning of Contained Reactants*)

Francis Fendell and Harald Rungaldier
Electro-Optics, Lasers and Research Center, Redondo Beach, California

Prepared under Contract NAS3-27264

National Aeronautics and
Space Administration

Lewis Research Center

February 1999

NASA Center for Aerospace Information
7121 Standard Drive
Hanover, MD 21076
Price Code: A04

Available from

National Technical Information Service
5285 Port Royal Road
Springfield, VA 22100
Price Code: A04

Table of Contents

	<u>Page</u>
Summary	1
Introduction	1
Main Discussion	3
(1) Experimental Design (Test Apparatus and Procedures)	3
(2) Test Preparation and Execution	
Recommendations	7
References	9
Figures	10
Appendix A	
1.0 Introduction and Summary: An Overview	A-1
1.1 Description of Experiment	A-1
1.2 Scientific Knowledge to Be Gained	A-9
1.3 Value of Knowledge to Scientific Field	A-10
1.4 Justification of the Need for Space Environment	A-11
1.5 Experiment Objective	A-13
2.0 Background	A-16
2.1 Description of the Scientific Field; Prior Research	A-16
2.2 Current Research and Its Applications	A-18
2.3 The Proposed Experiment	A-20
3.0 Justification for Conducting the Experiment in Space	A-26
3.1 Limitations of Ground-Based Testing	A-26
3.2 Limitations of Mathematical Modeling	A-27
4.0 References	A-32



Table of Contents

	<u>Page</u>
Summary	1
Introduction	1
Main Discussion	3
(1) Experimental Design (Test Apparatus and Procedures)	3
(2) Test Preparation and Execution	
Recommendations	7
References	9
Figures	10
Appendix A	
1.0 Introduction and Summary: An Overview	A-1
1.1 Description of Experiment	A-1
1.2 Scientific Knowledge to Be Gained	A-9
1.3 Value of Knowledge to Scientific Field	A-10
1.4 Justification of the Need for Space Environment	A-11
1.5 Experiment Objective	A-13
2.0 Background	A-16
2.1 Description of the Scientific Field; Prior Research	A-16
2.2 Current Research and Its Applications	A-18
2.3 The Proposed Experiment	A-20
3.0 Justification for Conducting the Experiment in Space	A-26
3.1 Limitations of Ground-Based Testing	A-26
3.2 Limitations of Mathematical Modeling	A-27
4.0 References	A-32



Summary

An effectively strain-rate-free diffusion flame constitutes the most vigorous laminar combustion of initially unmixed reactive gases. Such a diffusion flame is characterized by a long fluid-residence time and a large characteristic length scale, and, were the flame planar, by high symmetry as well. Such a diffusion flame is particularly suitable for the investigation of phenomena such as multicomponent diffusion, and the rates of soot (or other particle) inception, growth, and oxidation. Unfortunately, such a diffusion flame is inaccessible in earth gravity (*e.g.*, in a counterflow-diffusion-flame apparatus) because of the onset of Rayleigh-Benard instability (sufficiently pronounced hot-under-cold stratification in the presence of buoyancy).

Accordingly, a specially dedicated apparatus was designed, fabricated, and initially checked out for the examination of a planar strain-rate-free diffusion flame in extended-duration microgravity. Such a diffusion flame may be formed within a hollowed-out squat container (25 cm x 25 cm x 9 cm), with isothermal, noncatalytic, impervious walls. A thin-metal-sheet separator is withdrawn, by uniform translation in its own plane, through a tightly fitting slit in one side wall. Thereupon, diluted fuel vapor (initially confined to one half-volume of the container) gains access to diluted oxygen (initially with the same pressure, density, and temperature as the fuel, but initially confined to the other half-volume). After a brief delay to permit limited diffusional interpenetration of fuel vapor and oxidizer, a line ignitor, located (in the plane of the withdrawing separator) along that side wall from which the trailing edge of the separator withdraws, spawns a triple-flame propagation across the 25 cm x 25 cm centerplane. A diffusion flame is emplaced in the centerplane; the subsequent travel and temperature of that planar diffusion flame may be tracked. Eventually, nearly complete depletion of the stoichiometrically deficient reactant (chosen to be the fuel vapor), along with heat loss to the container surfaces, effects extinction.

Introduction

A flight-experiment project entitled "Unsteady Diffusion Flames: Ignition, Travel, and Burnout" was initiated, as one of the combustion-science tasks of the NASA Microgravity Science Research Program, on July 10, 1994 (project ID: 963-15-00). The principal investigator, and principal performer of theoretical tasks, was Francis Fendell of the Space & Technology Division of TRW Space & Electronics Group, Redondo Beach, CA; and the principal performer for TRW for experimental tasks was Harald Rungaldier, a staff member of the same division. A counterpart technical effort on the project was simultaneously initiated and pursued at the responsible center, the NASA Lewis Research Center (LeRC): the project scientist, and principal performer of theoretical tasks at NASA, was Suleyman Gokoglu of the Microgravity Combustion Science Branch of the Microgravity Science Division; the project experimentalist, and principal performer of experimental tasks at NASA, was Donald Schultz of the Experiments Definition Branch of the Microgravity Science Division. Funding for the LeRC portion of the effort, sustained under the Space Station Utilization budget, was effectively terminated around December 1996. Donald Schultz retired from NASA around April 1997 and later

contributed to the project as an employee of Westwind Engineering of Manhattan Beach, CA, under a subcontract from TRW. A proposal submitted by TRW in January 1998 in response to NASA Research Announcement NRA-97-HEDS-01 ("Microgravity Combustion Science: Research and Flight Experiment Opportunities"), to fund follow-on work on this project, was declined for support. This report documents the progress achieved during the nominal four-year period of performance that terminated on December 10, 1998.

This project concerned the design, fabrication, instrumentation, and checkout of a dedicated, novel combustion chamber (intended as a first cut at hardware ultimately suitable for spaceflight, to make use of the extended testing time in microgravity available on the Space Station). This hardware (Fig. 1) was conceived and studied as a means to: (1) emplace a planar, virtually strain-rate-free diffusion flame within an effectively impervious, isothermal, noncatalytic squat rectangular-solid container; and (2) track the position and properties of such a flame until extinction. Such a diffusion flame has high geometric symmetry (for experimental and mathematical simplicity), and is characterized by exceptionally large spatial scale (for experimental accessibility) and by exceptionally long fluid-residence time (an advantage for studying rates of sooting processes -- inception, growth, coalescence, and oxidation under flame-type conditions). Because of Rayleigh-Benard instability (the rapid growth in time, to disruptive magnitude, of inevitably present, small disturbances, owing to unstable, hot-under-cold stratification), no such planar, strain-rate-free diffusion flame is accessible in earth gravity. For example, it is well known that a counterflow apparatus is unable to stabilize a planar diffusion flame in earth gravity for strain rates smaller than about 20 sec^{-1} (Fig. 2). Thus, the experiment offers an opportunity to probe the fundamental aerothermochemistry of diffusion flames with fuels such as hydrogen, natural gas, and propane, which are gaseous under atmospheric conditions. This mode of combustion characterizes how most fuel vapor is burned, in both applications related to heating, manufacturing, boiling, and propulsion, and in uncontrolled, free-burning fire in structures and wildland vegetation. That is, this project sought to utilize microgravity testing to elucidate commonly encountered phenomenology, arising in the commonly encountered mode of combustion, of those commonly utilized fuels usually categorized as gaseous fuels.

Progress on the novel test apparatus for the proposed experiment did not reach the stage of permitting the collection of data in a ground-based microgravity facility (drop tower). Thus, no Science Concept Review (SCR) was held. Nevertheless, the format of the Science Requirements Document (SRD) normally prepared in conjunction with the convening of an SCR well serves the purposes of presenting relevant background (*e.g.*, what tradeoffs led to the adopted design, how the work relates to other investigations reported in the literature, which parametric assignments appear to warrant priority, which measurements seem readily accessible, and how the anticipated data could be used to upgrade modeling of diffusion flames). Thus, in the format of a self-contained SRD, Appendix A presents both the justification for the large investment inherent in testing in extended-duration microgravity and relevant scientific background, and the reader is taken to be familiar with that material. Appendix A also includes citations of all peer-

reviewed publications generated by the participants in the course of pursuing the investigation. A progress report was prepared for the Third International Microgravity Combustion Workshop (Fendell and Wu 1995) and for the Fourth International Microgravity Combustion Workshop (Fendell *et al.* 1997). The main text is dedicated entirely to details of the test apparatus, test procedures, preliminary results of testing, and suggestions for further effort, were additional work to achieve the objectives of the project to be undertaken.

Main Discussion

(1) Experimental Design (Test Apparatus and Procedures)

Even with a microgravity level of $g = 10^{-5} g_0$, where g_0 denotes the magnitude of earth gravity, the constraint imposed by a critical Rayleigh number of 1000 imposes a limit in height of about 9 cm for the primary (*i.e.*, test) chamber of the apparatus. That is, in microgravity, if an intense diffusion flame of temperature of about 2100 K lies in the centerplane of the primary chamber [so that the relatively cold impervious top surface lies 4.5 cm above (and parallel to) the centerplane, and the relatively cold impervious bottom surface lies 4.5 cm below (and parallel to) the centerplane], then the planarity of the diffusion flame is not disrupted by buoyant instability. These values are somewhat conservative because the Rayleigh-Benard problem (Fig. 3) has not been rigorously treated for the specific context of interest. The length and breadth of the horizontal cross-section of the primary chamber is taken to be 25 cm x 25 cm, in view of: (1) the time scale for the diffusive growth of near-side-wall quench layers into the core of the chamber; (2) the size of the apparatus that fits inside existing drop towers; and (3) the weight of apparatus that meets weight limitations of drop rigs in such drop towers.

About one second is required for: (1) the removal [by translation, at (ideally) constant speed, in its own plane] of a thin (~ 0.9 mm) metallic separator, so that the contents of the upper half-volume (say, 85% O₂, 15% He) and the contents of the lower half-volume (say, 35% H₂, 65% Ar) may begin to interpenetrate by diffusive transport; and (2) the propagation of a triple flame through the combustible mixture that forms near the centerplane of the primary chamber (Figs. 4 and 5). Thus, in about one second, a diffusion flame is emplaced across the entire centerplane of the squat rectangular-solid primary chamber (of stainless steel, with walls 1.25-3.27 cm thick); tracking the subsequent travel and properties of this diffusion flame is the key objective of the experiment. This travel, until extinction occurs, may require 10-30 seconds or more, depending on the reactant species and test conditions. Thus, the (say) two-second testing time available in a drop tower permits only the initiation of the experiment (essentially, the emplacement of a planar diffusion flame across the centerplane of the primary chamber); subsequent data collection on diffusion flame travel and extinction requires testing in prolonged microgravity (Figs. 6 and 7).

Incidentally, the thin metallic separator is removed from the primary chamber through a tightly fitting slit in one side wall of the container, and is stored in a 38 cm x 25

cm secondary chamber (to meet the requirements for providing housing for the pneumatic pulling mechanism for the separator). The separator must be so stored to permit redeployment in the primary chamber for a subsequent test (without breaking the pressure seal of the container, so leak-testing need *not* be repeated before each experiment). A separator sufficiently thick to preclude premature interpenetration is *not* satisfactorily rolled up in storage and then redeployed. Also, after an appropriate delay following the initiation of separator withdrawal, a combustible mixture of finite width is formed near the centerplane (aft of the trailing edge of the withdrawing separator). Then ten equispaced electrode pairs, aligned in the centerplane and sited near the side wall *opposite* to the slit-containing side wall, are simultaneously sparked to initiate the triple-flame propagation.

Nominally the contents of the two equal half-volumes are to be at atmospheric pressure (± 100 Pa) and temperature (± 10 K), and to have equal density ($\pm 0.1\%$), so that the "average molecular weight" for each half-volume is nearly the same. (The "average molecular weight" is about 29 for the above-cited reactant compositions.) The overall contents are to be sufficiently fuel-deficient that, if (conceptually) the initially segregated contents of the primary chamber were mixed to form a perfectly homogeneous gaseous mixture, the equilibrium burned-gas temperature under adiabatic burning would be consistent with a vigorous flame, but not so hot that dissociation of product species or gaseous radiative heat transfer or the physical integrity of the container is of concern. In Appendix A, attention is focused entirely on argon-diluted hydrogen as the contents of the fuel-containing half-volume, and helium-diluted oxygen as the contents of the oxygen-containing half volume; such a choice gives soot-free burning under relatively well-understood chemical kinetics, with appreciably differing mass diffusivities. While such reactants are characterized by conveniently wide flammability limits and ease of ignition, a consequence is that NASA regulations require extraordinary safety precautions. Further, the H_2/O_2 flame is invisible (so infrared sensors are required). The testing performed to date has concentrated on the argon-hydrogen/helium-oxygen pair. However, substituting methane for hydrogen permits investigation of another fuel of practical interest, one typified by typically modest sooting in diffusion-flame burning, by relatively well-studied kinetics, and by differing diffusivity relative to oxygen (though, of course, less differing than hydrogen). Furthermore, conveniently, the methane/oxygen diffusion flame is visible, and is either pale blue (detectable chemiluminescence, in the absence of sooting) or yellow (sooting). The methane/oxygen pair has narrower flammability limits, and less ready ignitability, than the hydrogen/air pair. If needed, a small amount of ethane (no more than one part in about twenty) might be added to the methane to facilitate ignition (as in natural gas).

Incidentally, nothing precludes extending any of the above-stated ranges for parameters. In particular, the peak post-burn pressure is reduced if the initial pressure is reduced, all other parameters being held fixed. However, decreasing the initial pressure to one-third of an atmosphere does enhance diffusion while decreasing the reaction rate, so the Damköhler number is reduced and the burning is more prone to being reaction-rate-limited. Still, the Reynolds number pertinent to separator withdrawal is invariant if the pressure is reduced to a third, while the speed of withdrawal (Fendell and Wu 1995;

Fendell *et al.* 1997) is tripled; then, less fluid is entrained by the separator (about a 40% reduction in volume), and less circulation is induced, while the propensity for transition to turbulence of the flow induced during separator withdrawal is unaltered. The flame speed for methane/air does increase with decrease of pressure, though decrease to one-tenth atmosphere barely doubles the speed; so the capacity of the triple flame to catch up to the wake of the withdrawing separator would be somewhat more challenging.

With the termination of the NASA-inhouse support, contractual resources were sufficient only for testing by allowing a carefully balanced platform with the experimental apparatus to fall freely in air for a distance of about five meters, onto cushioning. Such a drop affords an approximately one-second-duration-microgravity testing interval, although the drag on the following rig owing to the presence of the ambient air does not permit achievement of the virtually body-force-free level attained during testing in highly evacuated drop towers. The planar-diffusion-flame emplacement across the centerplane of the primary chamber could be achieved, were separator removal, spark ignition, and triple-flame propagation completed within that interval. In contrast, the onset of Rayleigh-Benard instability is expected to disrupt the planarity of the diffusion flame in less than one-quarter second in earth gravity; total removal of the separator requires about one-quarter second, lest shear-flow instability from too rapid removal disrupt the laminar flow.

Although windows are provided at multiple sites on the primary-container walls for optical access into the interior, the only diagnostic probe to be used during testing were pressure transducers, with kilohertz sampling rate adopted. Since reverberation of acoustic waves equilibrate the pressure field within the 9-cm-high primary container in a small fraction of a millisecond, the pressure field is anticipated to be spatially uniform to excellent approximation during virtually the entire one-second test, so the particular location (within the primary chamber) of the pressure probe is not crucial. Two identical pressure probes were installed for redundancy; both were placed in the midplane, one at a side wall and the other 12.5 cm away, at a site halfway across the chamber. Preliminary testing to satisfy safety requirements indicated that the multispark ignition system, chosen to achieve a line-type ignition at midheight along one face (of the 25-cm-square cross-section of the box), resulted in a pressure rise within roughly 10 milliseconds, from one-atmosphere initial pressure to about adiabatic-deflagration level (roughly six atmospheres), for an initially *homogeneous* room-temperature mixture, of appreciably fuel-lean equivalence ratio, in the primary chamber. That is, if the initial contents of the half-volumes of the container (prior to separator removal) were uniformly mixed so that the equivalence ratio were about 0.2 (a condition arising if the contents of one half-volume were roughly one-third hydrogen and two-thirds argon by mole fraction, and the contents of the other half volume were roughly four-fifths oxygen and one-fifth helium, and the separator were removed to permit the contents of the half-volumes to mix well), a significant pressure rise follows localized ignition in just 10 milliseconds or so. If a comparably large, comparably rapid increase in pressure is recorded by the pressure transducers during the triple-flame propagation through the stratified mixture in the primary chamber during the early, diffusion-flame-emplacement stage of a test in microgravity, then we may infer that the narrow horizontal strip of combustible mixture

(*i.e.*, mixture with local stoichiometry between the fuel-rich and fuel-lean flammability limits) has been disrupted by instability. Instead of an exothermic chemical reaction being confined to a narrow horizontal strip, an instability must have entered to cause deep, disruptive, finger-like intrusions of diluted hydrogen into the initially diluted-oxygen-containing half-volume, and intrusions of diluted oxygen into the initially diluted-hydrogen-containing half-volume. The readily-measured time history of the pressure field provides an average over the primary-chamber volume of the heat gain by the contents from the release of chemical exothermicity, minus the heat loss to the cold container walls. (The container walls, because of their large thermal inertia and high conductance, relative to the corresponding values for the gaseous contents, remain virtually isothermal at their initial room-temperature values.) Alternatively, if the pressure rise associated with diffusion-flame emplacement is measured to occur over a time interval consistent with the speed of combustible-mixture formation by shear-flow-enhanced interdiffusion and triple-flame propagation across the midplane (on the order of hundreds of milliseconds), then we may infer that no such disruptive instability has occurred. In fact, we then may reasonably infer that the design of the experiment admits, under microgravity, the smooth emplacement of a planar diffusion flame.

At the end of the microgravity testing time, when the container is suddenly decelerated by impact with the cushioning at the bottom of the fall, and burning initiated in microgravity continues in earth gravity, we expect the planar diffusion flame to be quickly and completely disrupted. We expect a rapid and significant rise in pressure, to confirm that not only can pressure transducers record such an event, but also the residual amount of unburned fuel vapor (chosen to be the species present in stoichiometrically deficient amount) is appreciable, and a longer microgravity-testing time is warranted for subsequent, data-collection experiments.

Two-dimensional unsteady numerical simulation of the triple-flame propagation through the combustible mixture formed (near the midplane of the primary chamber) aft of the trailing edge of the withdrawing separator was carried out by Suleyman Gokoglu with a modification of the computer code FLUENT. The simulation considers an exothermic flow in a closed container, with the characteristic acoustic speed far in excess of the characteristic advective speed, while an intrusive solid surface is being withdrawn at finite rate from the interior of the domain. Undertaking such a simulation places high demands on spatial and temporal resolution, and on numerical-grid adaptation, for accurate simulation of the physical processes; *e.g.*, accumulation of even minute errors in the pressure-field estimation can result in the abrupt onset of catastrophic flow-instabilities that are purely numerical artifacts. Inadequately refined grids in the vicinity of relatively cold container walls can result in artificially enhanced growth of reaction-quench layers. The early simulations did indeed indicate the onset of a disruptive instability during diffusion-flame emplacement, but no such instability arose in subsequent, higher-resolution calculations carried out by Dr. Gokoglu. In these more refined calculations, the diffusion flame retained a nearly planar geometry throughout the emplacement.

(2) Test Preparation and Execution

The container was assembled and tested for leaks and structural integrity. Some facility with the piston-in-cylinder separator-removal mechanism, the gas-filling procedure for the container, the O-ring seal pressurization, the spark-discharge timing for ignition, and the data recording for the pressure taps was achieved. A complete multi-tier drop package, including batteries for power and lines for data read-out, was designed and put together; the weight-distribution of the rig was balanced, and a smooth release of the drop rig from a supporting bolt was accomplished.

While many other subsystems were found to be operational at less than optimal levels (as discussed below), attention is focused on the inflatable seal, designed to prevent inappropriate mass transfer between the contents of the half-volumes, and inappropriate mass transfer from the primary chamber, in which the burning is conducted, to the secondary chamber, in which the withdrawn separator is stored, prior to redeployment in the primary chamber for the next test. The inflatable seals used in the testing under discussion were fabricated from pieces which were joined; almost every one of these seals proved too leaky for satisfactory use in a scientific apparatus. An inflatable polymeric *one-piece* seal that (1) is more resilient to leakage, even with one-atmosphere pressure difference across the membrane, and (2) fits into the groove provided in the container, is to be sought from suppliers prior to any further testing. In fact, a manufacturer who can furnish a leakfree seal has already been identified.

These challenges, together with the inevitable "learning curve" with a novel experimental apparatus, resulted in the occurrence of a significant operational failure during most tests, so only a limited amount of experimental data was obtained. Automation of the ignition sequence is planned in the future to remove one major source of operational failure; it proved impossible to achieve manually the desired split-second timing of sequential events (initiation of shutter pull, ignition, *etc.*).

The chamber typically was evacuated to a pressure of about 0.2 torr, and then filled to slightly below one atmosphere with initially segregated reactants. The pressure differential across the thin separator did not exceed 0.5 torr during the filling. Interchanging the contents of the half-volumes, so that the upper half-volume (usually containing hydrogen/argon) contained oxygen/helium instead, had very modest effect on results.

For a benchtop test (in earth gravity) in which the separator was removed by translation at 0.8 m/s across the 25-cm-wide primary chamber, and the contents of the half-volumes were allowed to mix for two minutes prior to ignition, then, subsequent to ignition, the pressure rose by about 60 psi in about 25 milliseconds. This result gives an indication of the magnitude and time scale for pressure rise in fairly-well-mixed gases, and is consistent with results of previous tests with very-well-mixed gases. The conclusion that the gases were fairly-well-premixed is based on the observation that the pressure increased only to 70 psi in about the same time span if the wait between separator removal and ignition was increased from two minutes to four minutes. The two

pressure taps yielded virtually identical pressure profiles as a function of time, as confirmation that acoustic waves do equilibrate spatial inhomogeneities in the pressure field, to excellent approximation.

For the only test executed in microgravity from which useful results were achieved, the pressure above one atmosphere is plotted as a function of time since initiation of the drop (Fig. 8). The vibration at release from the bolt, and the pressure disturbance at ignition 250 milliseconds later, are recorded; ignition was manually triggered just as the trailing edge of the separator plate clears the primary chamber, since the separator was translated at very nearly 1 m/s in this test. However, owing to human error in managing the recording devices, no detailed pressure trace is available until 500 ms after the start of this test. However, thereafter the continuous pressure trace indicates a smooth increase to a local pressure peak of about 66 psi (above the initial pressure) at 570 milliseconds. The pressure decreases, but slightly, to 61.5 psi (above the initial pressure) at 1050 milliseconds; at this time, the well-balanced package smoothly impacts the cushions at the base of the drop facility, with a deceleration measured to be only 20 *g*. As evidence that substantial hydrogen remains to be burned (in view of the highly fuel-deficient conditions of the test), the pressure rises to nearly 83 psi (above initial) at 1150 milliseconds, before decreasing monotonically -- presumably owing to heat loss from the contents to the container walls. At two seconds, even with appreciable churning of the contents of the chamber for 0.85 second, the pressure is still nearly 50 psi (above the initial pressure).

On the basis of theoretical modeling, we conjecture that the pressure monotonically rises to a peak as the area of the diffusion flame during emplacement, and the effects of compression from confinement of a suddenly formed mass of hot expanded product species, increase; the pressure then decreases slowly as the transport of fresh reactant to the emplaced diffusion flame begins to fall off owing to reactant depletion. The pressure decline at early time is expected to be particularly gradual because of the enhancement of diffusive transport by organized, recirculatory flow created by the withdrawal of the separator. The large positive derivative of the pressure as a function of time at 500+ milliseconds is consistent with a monotonic rise in pressure during the interval from 250 to 500 milliseconds. Unless the triple-flame-propagation speed exceeds 50 cm/s, the triple-flame propagation across the chamber is not convectively assisted during its transit of the chamber. Even the effective trailing edge of the separator-plate wake is already one-third the distance across the chamber at the time of the (delayed) ignition, and the triple flame may never catch up with the effective trailing edge of the wake. Thus, this test was not optimal in that the diffusion flame probably was not emplaced virtually as soon as the trailing edge of the separator was withdrawn from the chamber. Trading off withdrawal speed, ignition delay, and effective stoichiometry of the reactants requires extensive testing experience. However, *the fundamental experiment concept and execution seem sound.*

Recommendations

We add to our previous suggestions (that a one-piece leakfree polymeric O-ring seal be sought and that the millisecond-scale timing of the test-initiation sequence be automated) the following recommendations.

First, the precise positioning (height) of the ten-electrode-pair line ignitor should be varied until we identify the minimum delay in spark timing that succeeds in achieving initiation of triple-flame propagation. *Delay* here refers to the elapse of time after the beginning of separator withdrawal from the primary chamber until spark discharge. Minute repositioning might reduce the required delay significantly, on the millisecond time scale of interest.

Second, upgrading of the electronics in the control console is needed, as evidenced by problems with some of the pressure transducers during the automated filling of the half-volumes of the primary chamber. Noise ought to be eliminated from the various relays and solenoids in the gas system. Noise spikes from the relays have prematurely triggered sparking, and, in fact, portions of the spark-trigger circuit should be reworked.

Third, execution of check-out testing with methane (perhaps with traces of ethane), rather than with hydrogen, as the fuel vapor should facilitate the data collection (because the flame will be visible), and NASA safety-permit problems will be appreciably alleviated. In fact, it may be argued that, by the substitution, scientifically much is gained, and perhaps much practicality is also gained, since natural gas is now, and seems likely to remain, for decades, of greater commercial significance than hydrogen.

Fourth, since we shall probably continue to use a pneumatic cylinder to withdraw the separator from the primary chamber, the current apparatus is about 5 cm too long to fit within the NASA Lewis Research Center two-second drop tower, and is perhaps slightly too heavy as well. (The apparatus was sized for the five-seconds-duration microgravity facility.) Resolution of these problems may entail: (1) some alteration of the drag shield and frame; (2) perhaps removal of one window access to the interior (there are several others); (3) perhaps not quite fully withdrawing the separator from the primary chamber [this procedure would be acceptable for a short-duration test, to demonstrate successful emplacement of a planar diffusion flame, rather than to collect data, and the small portion of the separator remaining in the primary chamber would help to dissipate any "moving-corner" vortices (Fig. 9)]; and (4) possible integration of the pull cylinder with the container (*e.g.*, by using the container wall as one end of the cylinder). There should be no negative consequence to inclining the apparatus at a model angle ($\sim 30^\circ$) to the horizontal, but we are hesitant to adopt this resolution.

References:

Fendell, F., and Wu, F. (1995). Unsteady planar diffusion flames: ignition, travel, burnout. *Third International Microgravity Combustion Workshop* (NASA

Conference Publication 10174), pp. 357-362. Washington, DC: NASA Scientific and Technical Information Program.

Fendell, F., Rungaldier, H., Gokoglu, S., and Schultz, D. (1997). Strain-rate-free diffusion flames: ignition, properties, and quenching. *Fourth International Microgravity Combustion Workshop* (NASA Conference Publication 10194), pp. 93-98. Washington, DC: NASA Scientific and Technical Information Program.

Liebman, I., Corry, J., and Perlee, H. E. (1970). Flame propagation in layer methane-air systems. *Combustion Science and Technology* **1**, 257-267.

Phillips, H. (1965). Flame in a buoyant methane layer. *Tenth Symposium (International) on Combustion*, pp. 1277-1283. Pittsburgh, PA: Combustion Institute.

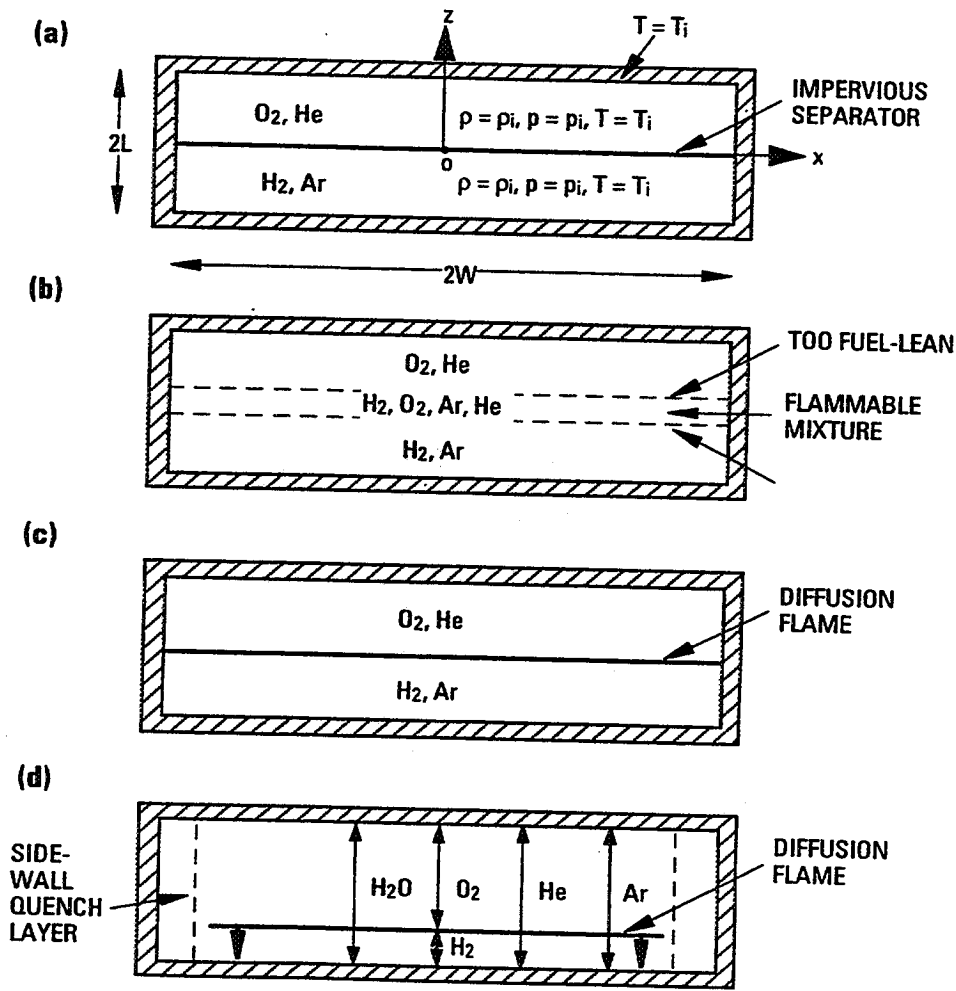


Fig. 1 Geometry for a planar translating strain-rate-free diffusion flame. (a) Helium-diluted oxygen and argon-diluted hydrogen occupy half-volumes in a squat container in microgravity. (b) Removal of the impervious separator with minimal disturbance initiates interpenetration of the reactants. (c) Timely ignition within the narrow layer of flammable mixture engenders a planar diffusion flame. (d) The planar diffusion flame typically travels into the half-volume with the deficient reactant (by choice, the fuel), as the cold-wall-quench layers thicken in time.

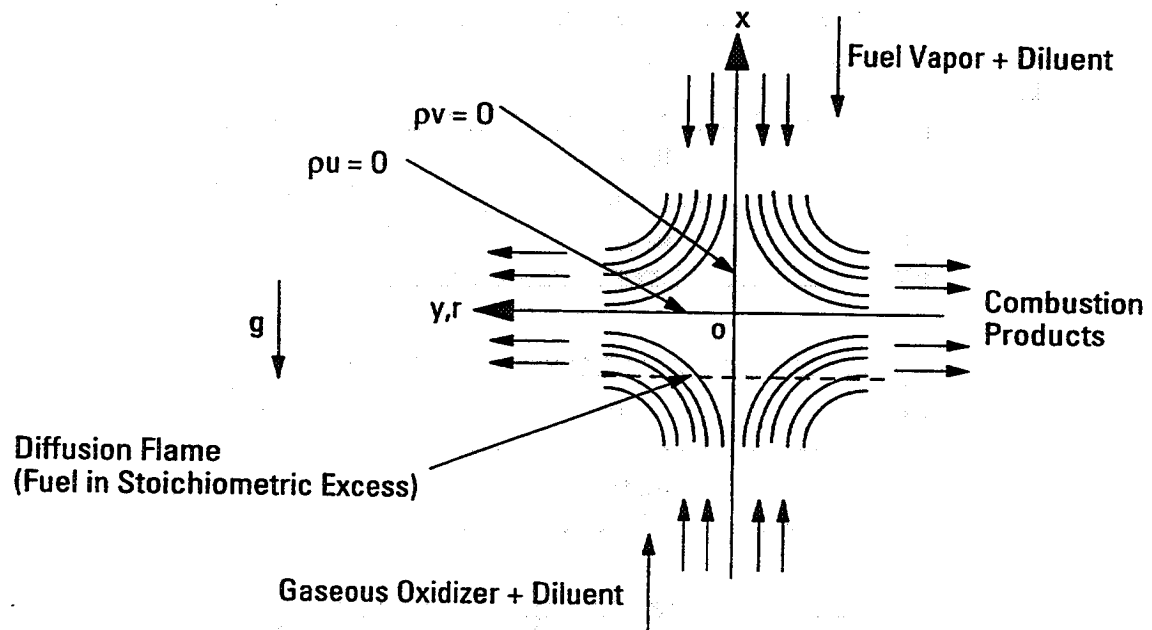


Fig. 2 In a steady counterflow of uniform opposed streams of fuel vapor and gaseous oxidizer, a planar diffusion flame can be stabilized in earth gravity, either in two-dimensional (x, y) or (cylindrically) axisymmetric (x, r) configuration. To excellent approximation, the axial mass flux ρu varies axially only, and the transverse mass flux ρv , transversely only. For $\rho u \rightarrow 0$ at large $|x|$, *i.e.*, as the ambient strain rate is decreased, fluid residence time increases; at sufficiently small strain rate, buoyant instabilities amplify to disrupt flame planarity in earth gravity.

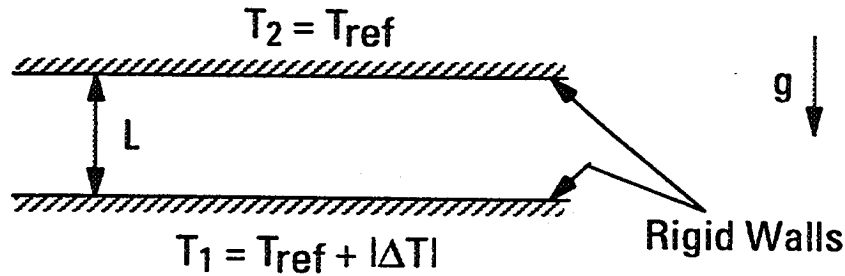


Fig 3 Classical Rayleigh-Benard instability concerns the onset of disruptive convection when one-dimensional diffusive heat transfer becomes unable to sustain hot-under-cold thermal stratification between parallel boundaries of separation L for gravitational acceleration g . The value of a dimensionless ratio of buoyant to diffusive forces, above which the onset occurs, is termed the critical Rayleigh number, and depends on the values of L , g , $|\Delta T|/T_{ref}$, fluid transport properties, and the physical nature of the boundaries. Thus, results are available for the modified problem involving a nonrigid lower boundary [which we identify with the diffusion flame depicted in Fig. 1, part (c), for design guidance].

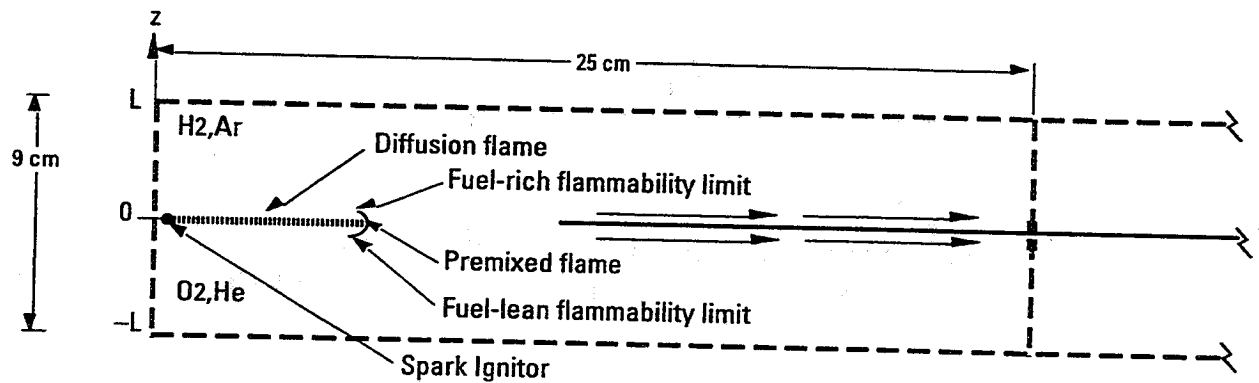


Fig. 4 A triple-flame propagates across the midheight plane of the primary chamber, through the stratified mixture formed aft of the trailing edge of the separator. The diffusion flame engendered by the triple flame remains planar in microgravity. The separator is withdrawn from the primary chamber [by translation (at approximately uniform speed) in its own plane] through a tightly fitting slit in a side wall; the separator is stored in a secondary chamber to permit subsequent redeployment in the primary chamber, without the need to break the container seal to conduct a sequence of tests.

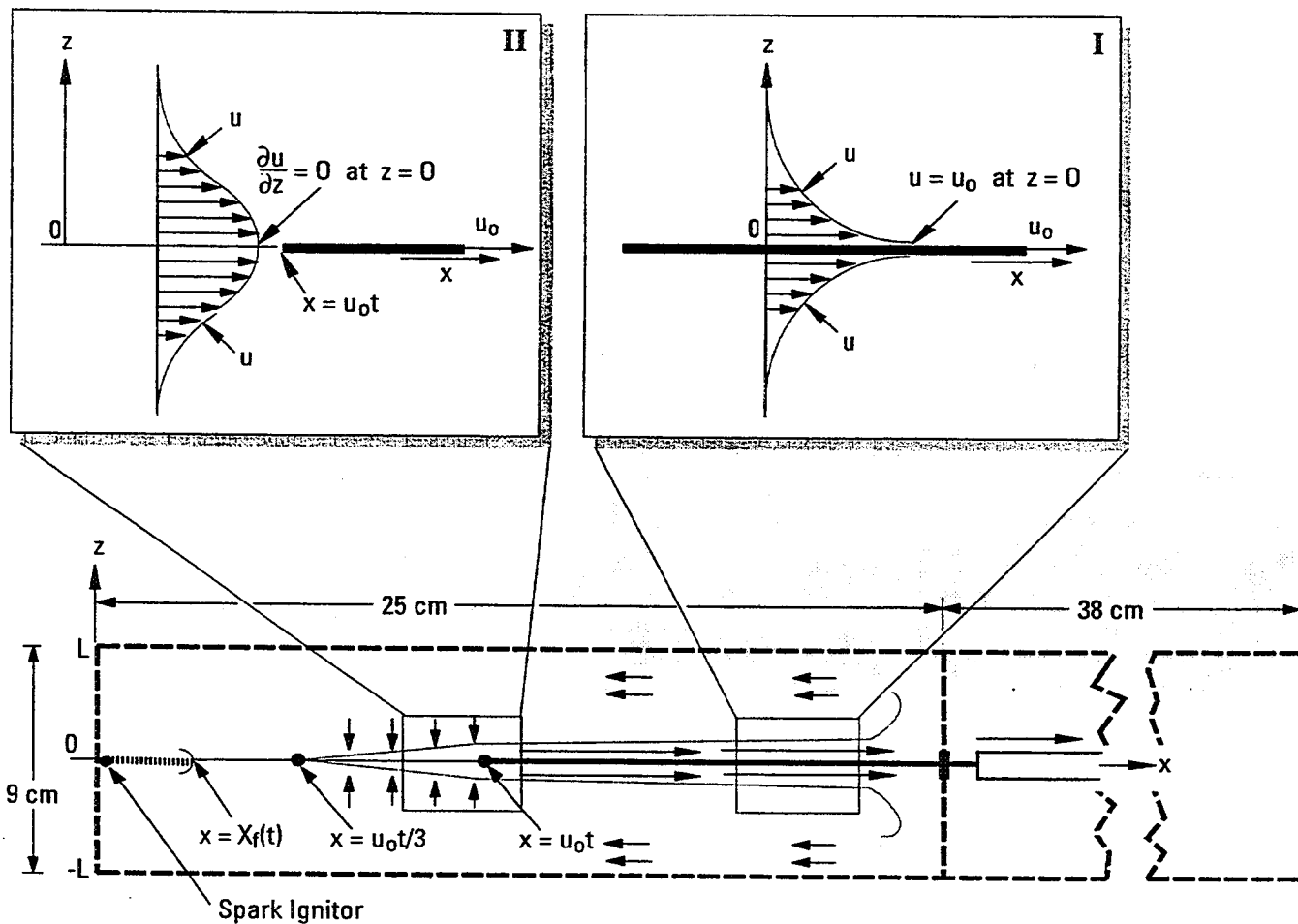


Fig. 5 The shear-flow dynamics associated with separator withdrawal at speed u_0 involves: (1) Rayleigh-type boundary layers induced on the top and bottom surfaces of the separator, and (2) a Gaussian-like profile for the streamwise velocity component in the wake, which is here approximated as extending for only a finite length behind the trailing edge of the separator.

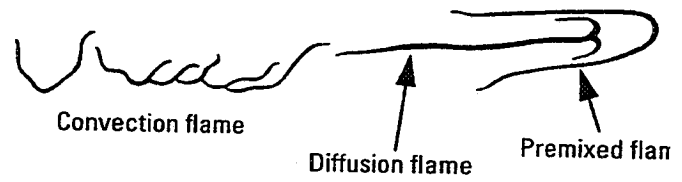
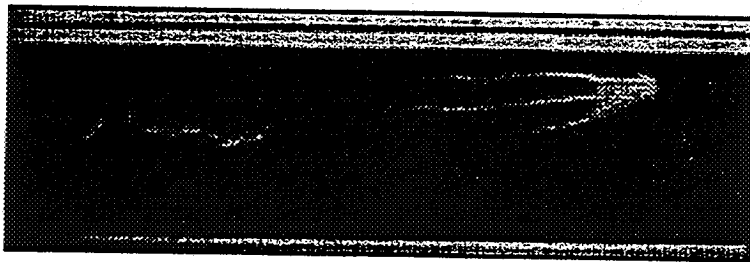
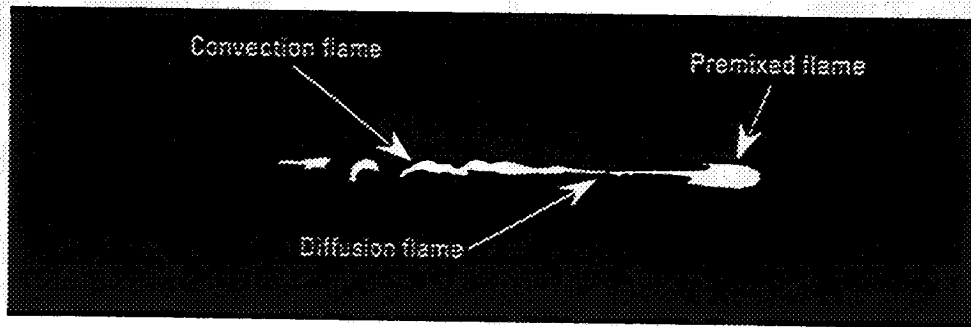


Fig. 6 Depiction of the rapid onset in earth gravity of convective instability, to disrupt the planar diffusion flame formed by triple-flame propagation through a stratified methane-nitrogen/air medium in a long gallery (Phillips 1965).



- In the frame of reference of the flame, with $S_U > S_{U_1} > S_{U_2} \dots$ and E denotes specific volume ratio across the flame

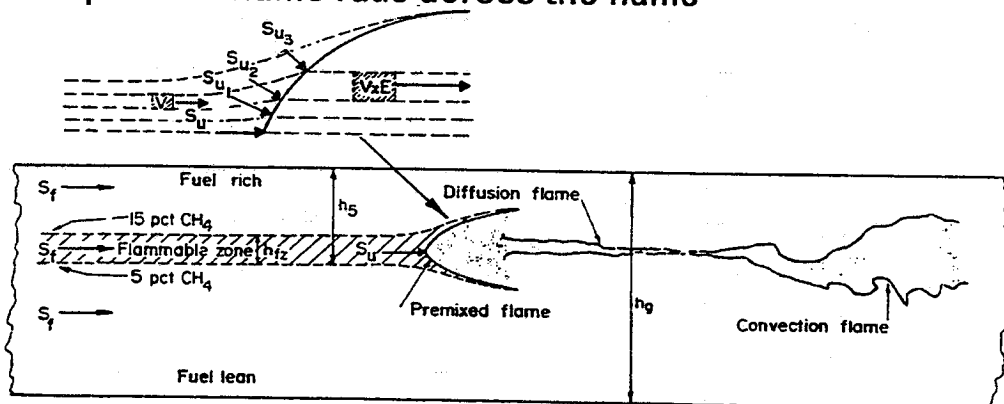
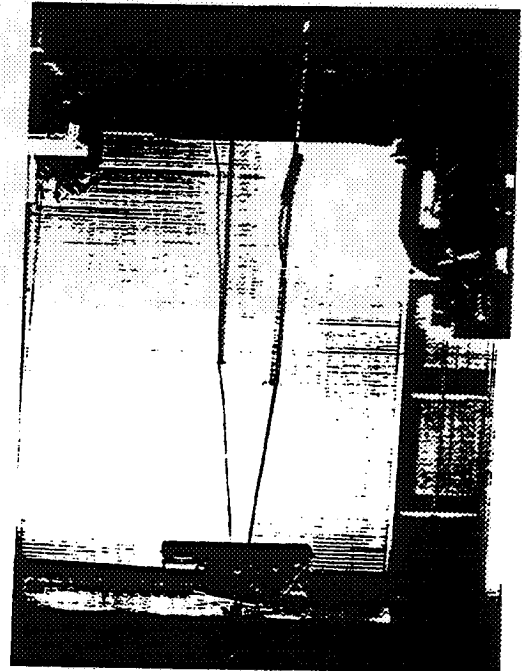
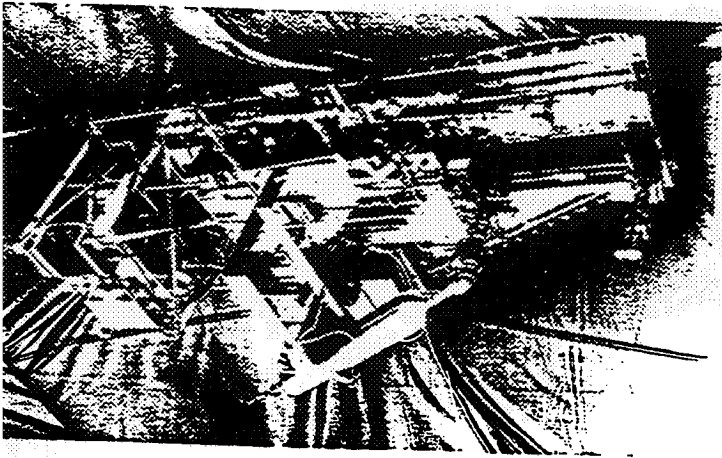
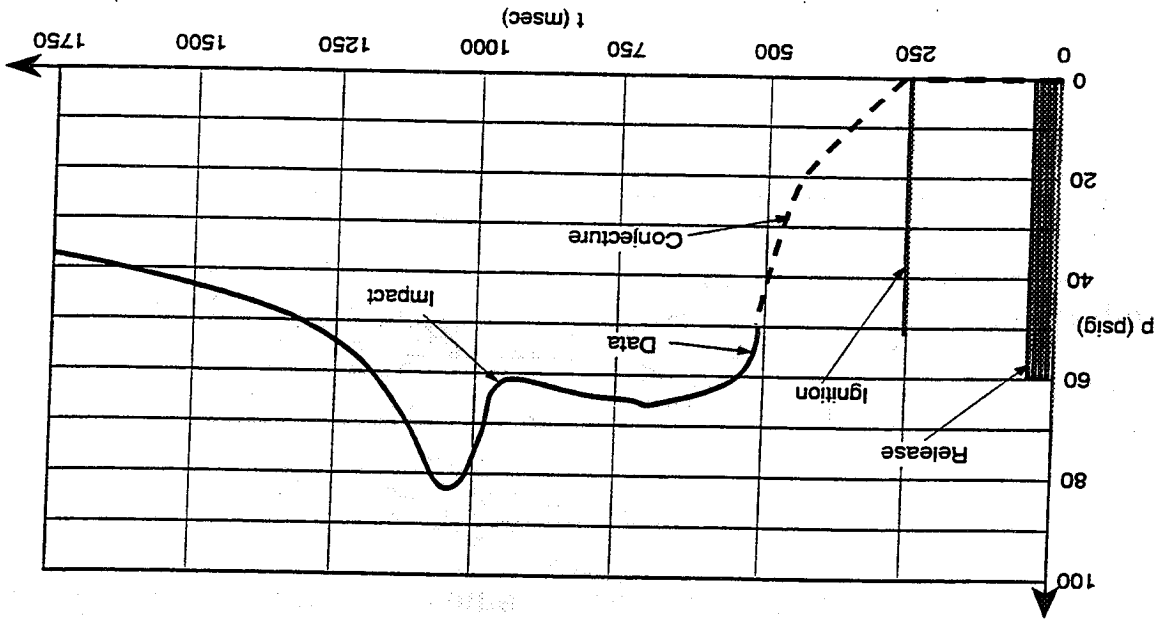


Fig. 7 An interpretative sketch by Liebman *et al.* (1970) of their photograph of convective instability rapidly disrupting the planarity of the diffusion flame formed by triple-flame propagation through a stratified methane/air mixture in earth gravity.

Fig. 8 The primary-chamber pressure (above the initial, ambient value) vs. time since the onset of separator withdrawal, during a one-second-duration test in microgravity in which the drop rig was released in a hangar. This test involved highly fuel-deficient conditions, in which helium-diluted oxygen and argon-diluted hydrogen occupied the half-volumes.



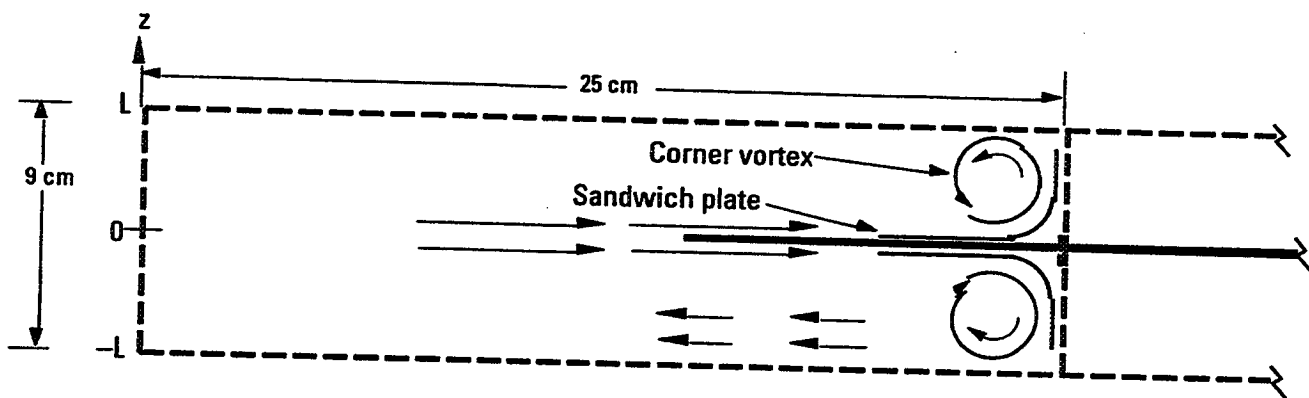


Fig. 9 Although a broad-drift return flow is depicted in Fig. 5 as the mode of redistribution of the fluid entrained by the withdrawal of the separator through the tightly fitting slit in a side wall, in fact, counterrotating "moving-corner" vortices may form above and below the midheight plane near that slit-containing side wall. Introduction of "sandwich plates" above and below the midheight plane would hasten the frictional decay of these vortices. Alternatively, for preliminary testing in brief-duration-microgravity ground facilities, the separator might be incompletely withdrawn to effect the same hastening of swirling-flow decay.



Appendix A

Science Requirements Document

for

Unsteady Diffusion Flames: Ignition, Travel, and Burnout

(SUBCORE Project: *Simplified Unsteady Burning of Contained Reactants*)

Combustion Science Program Project 963-15-00

**NASA Microgravity Science Research Program
Microgravity Science Division
NASA Lewis Research Center
Cleveland, OH 44135-3191**

**NASA LeRC Contract NAS3-27264
TRW S/N 62564
July 11, 1995 - December 10, 1998**

**Sensors, Lasers & Research Center
TRW Space & Electronics Group
Redondo Beach, CA 90278**



1.0 INTRODUCTION AND SUMMARY: AN OVERVIEW

1.1 Description of Experiment

1.1.1 Achieving High Symmetry to Facilitate Investigation of a Diffusion Flame

Steady one-dimensional deflagrations (Bush and Fendell 1970; Zeldovich *et al.* 1985) have been stabilized on heat-sink-type, flat-flame burners for at least four decades (Gaydon and Wolfhard 1979; Carrier *et al.* 1978); the planar simplicity of such nearly isobaric flames has availed both modelers and experimentalists in the study, even within earth gravity, of such topics as the effect of stoichiometry and dilution on the yield of environmentally sensitive trace species, including air toxicants, soot, and NO_x .

Another commonly encountered mode of combustion, e.g., in the context of engineering design for heating, manufacture, power generation, propulsion, etc., and in the context of uncontrolled burning in the form of wildlands fires, fuel-depot fires, structural fires, etc., is the burning of initially segregated fuel and oxidizer, such that the reactants coexist only at the interface at which exothermic chemical conversion to products species occurs. However, achieving a planar diffusion flame --the counterpart, for the burning of initially segregated reactants, of the flat flame achieved with a heat-sink-type burner for fuel/oxidizer mixtures--has been a challenge. The epochal work for diffusion flames was developed seven decades ago by Burke and Schumann (1928) in terms of a *multidimensional* concurrent-jet-type flow, in which a stream of one gaseous reactant (*e.g.*, the fuel) is enveloped by a stream of the other gaseous reactant (*e.g.*, the oxidizer). The adequacy of their highly approximate, perhaps overly simplistic modeling, which (for tractability) ignored the significant contribution of buoyancy, remains a subject of research even today.

One major advantage afforded by microgravity is the virtual elimination of the gravitational body force, to assist in the design of experiments of high symmetry. The advantage is, of course, the reduced need for diagnostic probing, and the relative simplicity of theoretical analysis.

In taking buoyancy $(\Delta\rho)g$ --where $(\Delta\rho)$ is a characteristic density difference and g is the magnitude of the earth gravitational acceleration--to be relatively negligible, we are comparing the magnitudes of two volumetric forces, $(\Delta\rho)g$ and $\rho_o v^2/L$, where ρ_o denotes a reference density, v denotes a reference speed, and L denotes a reference length. For a relatively high-

speed flow, the just-defined buoyancy/inertia ratio, $(\Delta\rho/\rho_o)gL/v^2$, the square of the inverse of the Froude number for a variable-density fluid, suffices as a criterion for the significance of buoyancy (Yih 1979). For a typical relatively low-speed flow in which no "impressed" speed v is readily identifiable, a diffusional speed is appropriate: $v \approx \kappa/L$, where κ denotes a characteristic diffusion coefficient; the pertinent ratio is between buoyancy and friction, and is termed the Rayleigh or Grashhof number $Ra \equiv (\Delta\rho/\rho_o)gL^3/\kappa^2$ (Yih 1979). [For typical gaseous systems, the Prandtl number $Pr(\equiv \nu/\kappa)$ is close to unity in value, and we have used this fact to take liberties in the above discussion.] Clearly, it is for larger-scale, lower-speed, more exothermic combustion phenomena that buoyancy enters significantly, to disrupt flows which otherwise would have high geometric symmetry. Among prototypical combustion phenomena, the benefits of experimenting in microgravity would be most evident for deflagrations and diffusion flames.

1.1.2 A Planar-Diffusion-Flame Experiment Feasible in Microgravity Only

Now envision an experiment in which the geometrically convenient, planar diffusion flame is achieved in a microgravity environment. We have a chamber in which the diffusion flame lies initially in the centerplane, $z = 0$, of an apparatus with cold noncatalytic impervious walls at $z = L$, the (say) top of the apparatus, and at $z = -L$, the bottom of the apparatus. The fuel vapor (and diluent) initially occupy one half-volume, say, $-L \leq z \leq 0$; the oxidizing species (and diluent) initially occupy the other half-volume, $0 \leq z \leq L$. The subsequent position and temperature of the diffusion flame then become key outputs of the experiment, for, in general, the diffusion flame will travel and have a different temperature in time. As a function of the diffusion coefficients of the reactants, the richness of the contents of the two half-volumes, and other parameters, the diffusion flame will lie at a position at which the diffusional fluxes of residual fuel vapor and oxidizer meet in stoichiometric proportion. Thus, the flame initially may move into one half-volume, then reverse its course and move into the other half volume; alternatively, the flame may monotonically travel toward one end wall, in pursuit of the stoichiometrically deficient reactant, until that deficient reactant is nearly totally depleted; alternatively, the diffusion flame may just hover in the vicinity of the centerplane indefinitely if: (1) the diffusional-transport coefficients of the reactants are equal, and (2) both fuel vapor and gaseous oxidizer are initially present in stoichiometric proportion.

1.1.3 Initiation of the Strain-Rate-Free Planar Diffusion Flame

In the previous section we have outlined the unsteady one-dimensional combustion phenomena that ensue from the travel of a planar diffusion flame initiated at the centerplane $z = 0$ of an enclosed noncatalytic isothermal impervious container with end walls at $z = L$ and $z = -L$, and with diluted fuel vapor in one half-volume ($-L \leq z < 0$) and diluted oxidizer the other half-volume ($0 < z \leq L$).

However, unless the fuel vapor and gaseous oxidizer are hypergolic (spontaneously combustible on contact), the formation of the planar diffusion flame at the centerplane of the chamber is a nontrivial undertaking. Generally, only exotic, caustic, and toxic gases constitute hypergolic bipropellant systems; we must examine the creation of the planar diffusion flame by the use of ignition devices, such as spark discharges, in a system with diluted hydrogen initially segregated from diluted oxygen (chosen for its soot-free simplicity). *In fact, demonstration of the capability to create a planar diffusion flame at the interface between the chamber half-volume containing diluted hydrogen and the chamber half-volume containing diluted oxygen is the major achievement sought for presentation at the Science Concept Review. Since the temporal interval for travel of a planar diffusion flame within the chamber typically requires a substantially longer testing time in a microgravity environment than is available in a ground-based microgravity testing facility, only demonstration of the feasibility of establishing the "initial conditions" for subsequent planar-diffusion-flame travel is possible in a ground-based facility.* While longer testing time in microgravity is available in an aircraft executing a Keplerian trajectory, the size of the testing chamber, the filling of the chamber, and the requirement for very low gravitational acceleration obviate the use of such an alternative.

For nonhypergolic reactants, we plan to remove a thin (millimeter-thick) but stiff and impervious sheet of light-weight metal (aluminum) by translation in its own plane, in a constant direction and at as constant a speed as feasible. We want to remove the separator so that we incur minimal disturbance (*e.g.*, owing to flutter, or transition to turbulence in the flow induced by the velocity of the separator, or the onset and growth of some other unidentified instability); such considerations suggest a slow rate of removal, say, $u_o = 50 \text{ cm/sec}$. We defer to the next section more detailed discussion of the side walls of the enclosed chamber; however, since a planar diffusion flame is sought, we seek a "squat" chamber of square cross-section $2W \times 2W$, with $2W \gg 2L$, where the height $2L = 9 \text{ cm}$. Weight, cost, and geometric constraints of existing ground-based microgravity-testing facilities limit $2W$ to 25 cm. Thus, it would take one-

half second, after the initiation of translation, for the trailing edge of the separator to clear the chamber, for the values just cited. While this is not an entirely trivial duration relative to the available microgravity-testing interval of 5 sec, it seems acceptable. However, we would be hesitant to accept an even slower speed of translation because, even at 50 cm/s, the reactants in the upper-half chamber and lower-half chamber have a half second longer to interdiffuse at (say) the left-hand side wall than do the reactants at the right-hand side wall; asymmetry in an ideally planar experiment is being incurred. Because all transport is predominantly diffusional, significant transverse gradients arise to smooth any asymmetry that arises in the core of the container; the tendency of the system is to eliminate (not to amplify) departure from planarity. The "selfcorrecting" smoothing occurs on the same temporal scale as the diffusion flame translates, so, if the disturbance causing nonplanarity is short-lived, the planar behavior is restored on a practically useful time scale. A faster rate of withdrawal is desirable (say, $u_o = 250 \text{ cm/sec}$, so withdrawal is completed in just 0.1 sec), if such a rate is compatible with laminar, relatively undisturbed flow and with mechanical design of the withdrawal device. The reason is that the volumetric entrainment of fluid along the withdrawing separator and in its wake varies as $u_o^{-1/2}$ (Fendell and Mitchell 1996), so, while the fluid entrained in the relatively thin boundary layers along both sides of the separator and in the wake of the separator flows faster for faster withdrawal, there is less fluid entrained. We expect the entrained fluid to encounter the right side wall and to turn toward an end wall (i.e., to the end wall at $z = L$ for fluid entrained from the upper-half volume, and to the end wall at $z = -L$ for fluid entrained from the lower-half volume). We then expect the fluid to return in the direction from whence it came, and to fill in for the entrained fluid to preserve continuity in the medium. However, whereas the fluid transport to the right was confined to a thin viscous boundary layer and wake, and rapid, the return flow to the left is broad and much slower. The consequence of separator removal from the chamber is the induction of an organized, counterflow-like enhancement, at early times, of the ideal, purely diffusional transport toward the centerplane; however, this enhancement is dissipated by diffusion, and (if necessary) can be accounted for in data interpretation. Some entrained fluid will inevitably end up in a more concentrated vortex near the centerplane and the right side wall, in each half volume; the axis of this vortex is parallel to the side wall and centerplane, and will decay fairly rapidly under viscous diffusion. Explicitly, the e -folding time for the decay of the vortical motion is $O[R^2/(\pi^2 \nu)]$, where ν is the kinematic viscosity of the gas

and R is the radius of the vortex (Fendell and Mitchell 1996); for $\nu = 0.1 \text{ cm}^2/\text{sec}$ and $R = 1 \text{ cm}$, that decay time is about 1 sec.

With the length $2W$ (of a side of the square-cross-section chamber) set to 25 cm, we may characterize what is acceptable departure from planarity of the diffusion flame. We seek to have the variation in the z -coordinate position of the flame, denoted z_f , to vary by no more than about 1% of the transverse (*i.e.*, x, y) expanse of the flame; for $2W = 25 \text{ cm}$, a limit of 1% variation implies that $|\delta z_f(t; x, y)| \lesssim 0.25 \text{ cm}$. In any case, a 4% departure from planarity, so that $|\delta z_f(t; x, y)| = O(1 \text{ cm})$, raises concerns because the entire travel in the z coordinate is, in general, limited to no more than 4.5 cm. These statements pertain to phenomena in the core of the chamber; the near-cold-wall quenching of combustion is discussed in the next section.

The reactants in the two half-volumes interpenetrate in the vicinity of the centerplane, aft of the trailing edge of the withdrawing separator; it takes roughly 4 msec or so for a combustible layer to grow to one-millimeter thickness in the z direction, after the trailing edge has passed a site in the centerplane. A combustible layer of several-millimeter thickness is expected to support a flame propagation. Ignition by sparking at multiple (say, at least ten) evenly distributed sites near the centerplane along the left side wall ($x = 0$) results in multiple flames that merge as they propagate. The flames cannot propagate far in the $+z$ or $-z$ directions, because, except in the near vicinity of the centerplane, the gaseous medium has local stoichiometry outside the fuel-lean and fuel-rich flammability limits, respectively. However, flame can propagate relatively rapidly in the transverse (*i.e.*, x) direction, especially near the centerplane, where the local gaseous mixture aft of the withdrawing separator is nearly stoichiometric. The upshot is that there is a flamefront, propagating in the x direction, that is crescent-configured (or umbrella-configured) in z , and corrugated in the y direction. Behind the crescent-configured propagating flame, *i.e.*, closer to $x = 0$, there is a diffusion flame, as any interdiffused reactants are burned off and the initially segregated contents of the upper half-volume and lower half-volume come into contact near the centerplane. What has been described is a well-known structure termed a triple flame, or three-branched flame (Phillips 1965; Liebman *et al.* 1970; Feng *et al.* 1975; Ishikawa 1983a, 1983b, 1983c); the structure is often encountered during the formation of a diffusion flame in initially segregated, nonhypergolic reactants. For example, in a long gallery of a coal mine, methane may accumulate near the ceiling and air near the floor, such that a spark within the flammable layer of the stratification results in the creation of a triple-

flame structure. Because of Rayleigh instability, the diffusion flame quickly becomes disrupted, but in microgravity the diffusion flame may remain planar. Flamespread in a stratified medium may be regarded as of fundamental interest in itself, and the chamber seems suitable for conducting such an investigation. However, attention here is focused on the travel of a planar diffusion flame, and flamespread in a stratified medium is scrutinized only because it is crucial stepping stone to the creation of the planar diffusion flame.

In fact, we seek as rapid a flamespread across the centerplane as is consistent with other, previously discussed constraints for the diffusion-flame initiation. We note that if the position of the trailing edge of the withdrawing splitter plate is $x = u_o t$, where $t = 0$ is the time at which withdrawal was initiated and where withdrawal at constant speed is postulated, then at $x \approx u_o t/3$ the speed of the centerplane flow in the wake of the withdrawing separator is reduced to quite small values. If the flame propagates at a speed $v_f > (u_o/3)$, then the propagating flame, even if ignited aft of the trailing "edge" of the wake, may catch up to the translating wake. If so, thenceforth, the speed of the flamefront in the x direction is the sum of the propagation speed v_f and the flow speed in the wake at the position of the flamefront. Thereupon, the flamefront may move across the breadth of the chamber *almost* at the speed of the plate--recall that it takes a finite time to form a flammable mixture (of sufficient thickness to support flame propagation) by diffusional inter-penetration aft of the trailing edge of the separator. The upshot is that, while we do not want to spark too soon after initiation of separator withdrawal, lest the spark be dissipated in a nonflammable mixture, we want to spark as soon as a combustible mixture in a sufficiently thick layer exists, so that there is minimal delay in having the flame "catch" the wake. In this discussion, we have not cited the expansion of the burned gas as a contributor to the translation of the flame across the centerplane. The reason is that we believe, on the basis of the geometry (specifically, the near-centerline confinement of the flame propagation) that the burned-gas domain expands primarily toward the end walls at $z = L$ and $z = -L$, not across the breadth of the chamber toward $x = 2W$, where the separator is withdrawn through an air-tight seal. This is a conservative approximation in that at least some assistance of the flamespread may be derived from burned-gas expansion, especially immediately after ignition by the line of sparks.

1.1.4 Side-Wall Quench Layers

Since the organized velocity associated with the predominantly diffusional motion in the chamber is negligible, we can disregard near-side-wall effects owing to viscous (no-velocity-slip) effects. In fact, the walls are well approximated as noncatalytic, so the species concentrations of

the planar-diffusion-flame solution holding in the core of the finite-cross-section chamber ought not be disrupted, to any appreciable extent, in the vicinity of the side walls. However, it would take adiabatic side walls for the thermal field in the core of the container to persist, without appreciable modification, to the side walls. In fact, the centimeter-or-more-thick stainless-steel walls of the container possess so much thermal inertia, relative to the roughly kiloJoule chemical energy of the chamber contents, that the walls remain effectively isothermal at their initial temperature. Hence, the planar diffusion flame is thermally quenched in the vicinity of the side walls. The thermal-boundary-layer thickness at the side walls increases in time, roughly as the diffusional distance, $2(\kappa t)^{1/2}$, where κ is recalled to denote a characteristic value of the thermal diffusivity and t denotes time since experiment initiation (Carslaw and Jaeger 1959). In fact, this spatial growth in time of wall-induced phenomena is the motivation for choosing the dimension $2W$ of a side of the square cross-section to be 25 cm. For the conservative assignment $\kappa = 0.2 \text{ cm}^2/\text{sec}$, the wall-quench layer has intruded about half way to the center of the container in about 50 sec.

The side-wall diffusion-flame-quench layer is essentially elliptic, not parabolic in nature, in that spatial gradients both normal to the side wall and parallel to the side wall are significant (Baumstein and Fendell 1998). In many scenarios involving near-wall diffusional layers, the phenomena occurring away from the immediate vicinity of the wall boundary are nondiffusive, and only those diffusional gradients acting perpendicular to the wall enter significantly in a near-wall boundary layer, to permit adjustment of the core flow to the wall constraint(s). In these scenarios, the core flow is inviscid, and the boundary-layer flow is parabolic (*e.g.*, for the description of the high-Reynolds-number, low-Mach-number flow past a semi-infinite flat plate, where we exclude the exceptional circumstances holding in the immediate vicinity of the leading edge of the plate) (Leal 1992). However, in the phenomena of interest here, conduction of heat in the z direction is central to the description of the planar diffusion flame in the core of the chamber. The constant-temperature constraint at the container boundary introduces, perpendicular to the side walls, local thermal gradients comparable in magnitude to the typical thermal gradients parallel to the side walls.

To good approximation, the near-side-wall quench layer is "chemically frozen" for a planar diffusion flame in the core of the container, because the fuel vapor and gaseous oxidizer do not interpenetrate. Later in a test, when the burning in the core is weaker and more diffuse, the fuel vapor and gaseous oxidizer may interpenetrate and coexist, both in the core and near the

side walls. However, if the rate of reaction between the initially segregated reactants is of reduced intensity in the core, the rate of reaction is even smaller in the side-wall quench layer, owing to the locally small value of the Arrhenius factor (Zeldovich *et al.* 1985). The temporal variation of the heat transfer to the side wall at a fixed position $z = z_I$ (say, as the plane of the diffusion flame approaches to, lies at, and then continues past the position $z = z_I$) may challenge the sensitivity of readily available diagnostic instrumentation. However, the temporally varying thickness of the diffusion-flame-quench layer contiguous to the side wall may be detectable. While measurement of properties of the quench layers is not currently planned for the space experiment, because other observations are regarded to be of greater scientific value, the additional phenomenology associated with the quench layers provides possible topics for future investigation.

1.1.5 Selecting Reactive Species for Investigation

We address specific choices of fuel-vapor/diluent and gaseous-oxidizer/diluent for testing in the planar-diffusion-flame apparatus. The chamber is intended to be suitable for studying a wide range of reactive systems; *e.g.*, the long residence time of fuel vapor near a diffusion flame makes the apparatus appealing for examination of sooting phenomena in initially segregated hydrocarbon-vapor and air systems, and of ceramic-particulate formation and growth in stock-gas-seeded diffusion flames (see Section 1.5).

However, at the outset we elect to concentrate on the sooting-free hydrogen/argon and oxygen/helium system. We may alter the proportion of hydrogen with respect to argon, the proportion of oxygen with respect to helium, and the "stoichiometry" (the proportion of hydrogen with respect to oxygen), such that the pressure, density, and temperature in one half-volume is equal to the corresponding quantities in the other half-volume, yet, if we were (conceptually) to mix homogeneously the contents of the two half-volumes and then deflagrate the mixture, we could achieve a wide range of adiabatic flame temperatures. Here we concentrate on significantly hydrogen-deficient contents, such that we expect excess oxygen after all (or, more meticulously, nearly all) the hydrogen has been converted to product species (predominantly water vapor). By choosing argon and helium as the diluents, we avoid the complications of "nitrogen chemistry" that often arise with the use of air. We reiterate that hydrogen-oxygen chemistry is well-studied, well-mastered, and simple, relative to hydrocarbon/air chemistry; furthermore, the system introduces significantly differing diffusivities for species and heat, an aspect of diffusion-flame phenomenology that has been

relatively neglected, but is physically intriguing, mathematically challenging, and (most importantly) practically relevant.

We also note that detecting the temperature and position of the effectively invisible hydrogen-oxygen diffusion flame is relatively demanding on (infrared) diagnostic instrumentation.

1.2 Scientific Knowledge to Be Gained

The transport of species and heat in the closed chamber is predominantly diffusional. We choose not to adopt forced-convective effluxes from opposed, specially designed exits, as in the counterflow (described in Section 1.5), for two reasons: (1) we are intentionally seeking to examine the strain-rate-free limit $D_1 \rightarrow \infty$, *i.e.*, a "pure" diffusion flame; and (2) we seek to avoid the complication of prolonged storing, steady feeding, steady collecting, and long-term disposal of gas that has traversed the counterflow domain, the accumulation of which within the counterflow domain would contaminate the experiment. The tradeoff is that we have an unsteady and nonisobaric, but still planar and laminar, diffusion flame. Monitoring the rise and fall of the effectively spatially uniform, but temporally evolving, pressure furnishes insight into the relative roles of chemical exothermicity (and perhaps some compressional heating), especially at early times, and heat loss to the walls (and perhaps some expansional cooling) at later times. *We believe that this experiment is one which Burke and Schumann (1928) might have proposed, had microgravity testing been available to them. Tracking and modeling the flame position and temperature in time in the proposed unsteady one-dimensional microgravity experiment is the (we anticipate, simpler) counterpart of tracking the flame position and temperature in space in the original Burke-Schumann steady two-dimensional buoyancy-affected laminar-jet-diffusion-flame experiment in earth gravity.* That is, if achieving solution is contingent on applying constraints on the continuity of dependent variables, and discontinuity of gradients of these variables, at a surface (the flame), the position of which is to be found in the course of solution, then one-dimensional buoyancy-free configurations are much more tractable than two-dimensional buoyancy-affected configurations (Section 1.3). *The proposed planar-diffusion-flame experiment is expected to furnish data to ascertain the adequacy of convenient approximations, straightforward extensions of those adopted by Burke and Schumann, to facilitate mathematical solution.*

1.3 Value of Knowledge to Scientific Field

The traveling planar diffusion flame in microgravity is of particular *mathematical* as well as physical interest. First, the experiment brings out the *moving-boundary-problem* (i.e., *Stefan-problem*) *property of the diffusion flame* (Carslaw and Jaeger 1959; Crank 1975, 1984; Hill 1987). The flame is the translating boundary between fuel vapor and gaseous oxidizer, the position and properties of which must be ascertained in the course of solution, as a condition of solution. In concentrating on highly idealized, equidiffusional scenarios and/or steady configurations, prior investigators have not addressed the moving-boundary-problem property of the generalized analysis of a diffusion flame; the position of the flame is fixed in steady scenarios, and that position may be found *a posteriori* from a directly obtained, composite (fuel-domain-and-oxidizer-domain) solution in equidiffusional scenarios. Second, as the stoichiometrically deficient reactant is depleted to exhaustion, or as both reactants are simultaneously depleted to exhaustion for reactants initially present in stoichiometric proportion, the rate of reactant conversion to product species per unit area of the planar diffusion flame decreases. Not only is the rate of transport of fresh reactant to the flame diminished, but (especially in view of the decrease of the flame temperature, for a reaction rate with large Arrhenius activation temperature) the rate of chemical conversion to product species of the fresh reactant that does arrive at the flame is diminished. The upshot is that, prior to the total depletion of the deficient reactant(s), the burning becomes less intense and less concentrated; the scenario alters from a diffusion flame to more diffuse burning of initially segregated, but now ever-more-interpenetrating fuel vapor and gaseous oxidizer (Section 1.5). Measurement of the residual amount of the stoichiometrically deficient species furnishes an indicator of the onset of finite-rate-chemical-kinetics effects prior to diffusion-flame extinction.

1.4 Justification of the Need for Space Environment

1.4.1 Rayleigh Instability

The reason that the nearly flow-strain-rate-free, molecular-transport-dominated diffusion flame is inaccessible in earth gravity relates to Rayleigh instability, the tendency of inevitably present, small disturbances to grow to planar-symmetry-disruptive magnitude in a short time, owing to buoyancy acting on a sufficient lighter-gas-under-heavier-gas stratification. While a slightly unstable stratification along the direction of the gravitational acceleration may be sustained by diffusional processes, such diffusional processes can be overwhelmed. Too

unstable a density stratification [such that a critical value $(Ra)_c$ of the above-defined Rayleigh number is exceeded] results rapidly in planar-symmetry-disruptive, finger-like intrusions of the lighter gas into the heavier gas, and the heavier gas into the lighter gas, as a naturally arising mechanism in response to nonuniformities in density that diffusion is insufficient to sustain (Goldstein and Volino 1995). The hot planar diffusion flame in a nearly isobaric counterflow engenders just such a lighter-gas-under-heavier-gas, highly unstable stratification; as discussed in greater detail in Section 1.5 below, by laboratory observation (*e.g.*, of a counterflow diffusion flame) gravitational instability grows to disruptive magnitude in no longer than about 0.2 sec, perhaps as rapidly as about 0.05 sec, in earth gravity. If the strain rate exceeds $a = O(20 \text{ sec}^{-1})$, then we may infer from observation that the rate of growth of convective instability is sufficiently prolonged relative to the residence time of a fluid blob within a laboratory-scale counterflow apparatus [$L = O(1 \text{ cm})$] that the blob leaves the “working volume” before the growth is disruptive of planar symmetry. However, for such larger values of the strain rate, the burning of initially segregated reactants becomes an ever poorer approximation of a diffusion flame. The precise value of the critical Rayleigh number has never been calculated for unpremixed combustion, because solution of a challenging, high-order eigenvalue problem is entailed. However, from known solutions for the critical Rayleigh number for the geometry of two parallel planes, the lower one being hot and stress-free, and the higher one being cold and rigid, we anticipate that (Goldstein and Volino 1995)

$$(Ra)_c = \left(\frac{\Delta\rho}{\rho_o} \frac{gL^3}{\kappa^2} \right)_c \approx 800 .$$

For pertinent conservative parameter values for a vigorous flame, *i.e.*, $(\Delta\rho/\rho_o) = 7$, $\kappa = 0.2 \text{ cm}^2/\text{sec}$, $g = g_o \approx 10^3 \text{ cm}/\text{sec}^2$, it is seen that, in earth gravity, a stable diffusion flame in a “strain-rate-free counterflow” entails experimentation in a millimeter-scale apparatus--not only extremely demanding diagnostically, but almost totally worthless anyway, because the volumetric phenomena of interest would be boundary-effects-dominated. In the microgravity environment achievable in earth orbit, the magnitude of the gravitational acceleration is decreased by five orders of magnitude, so $g \approx 10^{-5} g_o$, such that $L \leq 4.5 \text{ cm}$ is still consistent with planar symmetry. For example, if a vigorous diffusion flame were to lie in the plane $z = 0$, and a planar boundary fixed at ambient room temperature were to lie at $z = L$, then the value of the critical Rayleigh number suggests that for $L \leq 4.5 \text{ cm}$, no planar-symmetry-disruptive

disturbances would arise. Such an experimental apparatus, while not indefinitely large, would be suitable for diagnostic probing.

The question arises whether, in earth gravity, we could so stably stratify the initially segregated reactants [e.g., by igniting a flame at the interface between an upper layer of hydrogen (possibly diluted with helium) and a lower layer of oxygen (possibly diluted with argon)] that the exothermicity of a diffusion flame does not disrupt planar symmetry. Since the product species is largely water vapor, with molecular weight intermediate to that of the hydrogen-helium and oxygen-argon layers, the question seems worthy of pursuit. Calculations show that, for the vigorous burning that characterizes a diffusion flame, the density profile with height quickly becomes unstable, in spite of the stable initial arrangement (Fendell and Mitchell 1996). A contributing factor is the interdiffusion of argon and helium, so that the background stratification is compromised on the same time scale as any other diffusional phenomenon taking place.

1.4.2 The Need for Extended Testing Time in a Microgravity Environment

The above-described strain-rate-free planar diffusion flame differs in substantial ways from other diffusion flames, previously studied in microgravity, even other diffusion flames describable in terms of a single spatial coordinate. First, the adoption of the planar-flame geometry conveniently eliminates the contribution (e.g., to diffusional transport) owing to curvature that arises in cylindrically symmetric and spherically symmetric flames. The spherically symmetric burning of a fuel droplet in a stagnant oxidizing atmosphere (Penner 1957) has long been a subject of microgravity experimentation (Microgravity Combustion Branch 1995); a more recent variant is the injection of a fuel vapor through a porous spherical surface into a stagnant oxidizing atmosphere. In the fuel-sphere geometry, there is net flux of mass radially outward through the spherical diffusion flame. In contrast, in the proposed strain-rate-free planar diffusion flame, there is negligible net flow through the plane of the flame; in fact, many cases of interest are characterized by a stagnation plane in the near vicinity of the diffusion flame. Thus, conventions appropriate for other diffusion flames [e.g., that a practically encountered fuel droplet of 10-20- μm size typically burns out within the 2-5-second testing time available in a ground-based microgravity-combustion facility (Microgravity Combustion Branch 1995; Committee on Microgravity Research ... 1995)] do not hold for the proposed experiment, even with all reactants initially present in the gas phase.

In the absence of a significant organized convective transport, the characteristic time scale for the strain-rate-free planar diffusion flame is the diffusive time scale, L^2/κ , where it is recalled that the half-height L of the chamber is 4.5 cm and the diffusivity $\kappa = 0.7 \text{ cm}^2/\text{sec}$ for diffusion of hydrogen, but only $0.2 \text{ cm}^2/\text{sec}$ for diffusion of heavier hydrocarbon fuels. The time scale to extinction might be as small as about 10 seconds for hydrogen as the fuel vapor, but as long as half a minute for a gaseous hydrocarbon as the fuel vapor. For the convenience of simply enumerated products of combustion, operation under fuel-deficient stoichiometry is anticipated. Thus, in the just-cited examples, effective exhaustion of the fuel vapor is taken to be the reason for planar-diffusion-flame extinction in the chamber.

1.5 Experiment Objective

We ask whether a planar diffusion flame can be established for the convenience of probing and analysis, via the effective freedom from buoyancy afforded by testing in microgravity. As noted previously and reiterated here, the probing of a planar diffusion flame should furnish definitive data to ascertain the adequacy of convenient approximations, generalizations of those adopted by Burke and Schumann, to facilitate mathematical solution. This is a simple, concise statement of the objective of this project. However, it is a deceptively simple statement, and requires extensive elaboration.

First, a planar diffusion flame can be created even in earth gravity, for some circumstances--a fact known for over three decades. In the counterflow geometry, the effluent from a properly designed outlet for fuel vapor is flowed against the effluent from a properly designed outlet for gaseous oxidizer, to create a selfsimilar planar diffusion flame. This is an aerothermochemical generalization of a classical exact steady solution to the Navier-Stokes equations for a Newtonian (viscous) fluid, discussed in many fluid-dynamic texts as the planar or axisymmetric stagnation flow: a simple ideal flow with constant but finite strain rate, effectively inviscid at large distances from a planar wall, encounters an impervious wall. By reflecting the flow in the one half space to the other half space, and by regarding the wall to be the stagnation plane for the axial velocity component only, we arrive at the counterflow with a planar diffusion flame. For equidiffusion, the flame situates itself at a plane parallel to the stagnation plane for the axial velocity component; the plane of the diffusion flame typically lies to the oxidizer side of the flow-stagnation plane if the gaseous-oxidizer flux at the oxidizer outlet is stoichiometrically deficient, to the fuel side if the fuel flux is stoichiometrically deficient, and at the stagnation plane itself if the two reactant-conveying streams are stoichiometrically balanced.

We designate the constant strain rate of the counterflow by the symbol a , with units of a frequency. A key dimensionless parameter of many aerothermochemical flows, including the counterflow, is the first Damköhler similarity group, or (simply) the Damköhler number, D_1 --the ratio of a characteristic flow time to a characteristic chemical-reaction time (Penner 1957; Friedlander and Keller 1963; Fendell 1965). We designate by the symbol B_f the effective collision-frequency factor of the chemical reaction rate, again with the units of a frequency. Hence, we may identify $D_1 \equiv B_f/a$. We infer that: (1) as $D_1 \rightarrow 0$, the residence time of reactants in the flow is shorter than the time required for exothermic chemical conversion to occur, and the flow is "chemically frozen"; (2) for $D_1 = O(1)$, chemical-reaction and fluid-"blob"-residence times are comparable, and a diffuse, moderately hot reaction zone exists in which fuel and oxidizer are converted to product species; and (3) as $D_1 \rightarrow \infty$, the chemical-reaction time is so much briefer than the fluid-transport time that there is vanishingly little interpenetration of fuel vapor and gaseous oxidizer--the reactants that reach a virtually mathematically thin interface (the flame) are there converted instantaneously to product species. It is this special last circumstance of an indefinitely thin ("structureless") reaction zone for which we meticulously reserve the description *diffusion flame*--since the constraint on the mass of conversion per unit area per time of reactant to product is provided by fluid transport only, and the dominant mode of transport of reactant species, product species, and heat in the immediate vicinity of the (aptly named) diffusion flame is diffusion. The peak temperature attainable in the flow field owing to chemical exothermicity occurs at the position of the diffusion flame. We meticulously reserve the description *burning of initially segregated reactants* for case (2) above, in which convection and diffusion are more nearly comparable for transport in the vicinity of a diffuse, cooler reaction zone, and for which chemical-kinetic rates as well as transport rates limit the rate of conversion of reactant species to product species.

Accordingly, the most vigorous burning of initially segregated reactants occurs in the diffusion-flame limit $D_1 \rightarrow \infty$. This is the particular case that interested Burke and Schumann. Mathematically, the diffusion flame is a singular limit in which the law of mass action becomes a Dirac delta function: the flame is a mathematical interface, which is a sink for reactants, and a source for product species and heat. Fluxes (normal to the flame) of reactants, products, and heat are discontinuous at the flame, but the temperature and mass fractions themselves are continuous at the flame. For the counterflow, the only geometry for which the burning of initially unmixed reactants displays planar symmetry for the mass fractions, the temperature, and the velocity

component perpendicular to the flame, the limit $D_1 \rightarrow \infty$ is approached, for testing with fixed reactants issuing at fixed thermodynamic state, for the strain-rate-free condition $a \rightarrow 0$. This is an experimentally appealing limit to investigate because the physical scale of the flow, $(\kappa/a)^{1/2}$, becomes large, and diagnostic probing is facilitated. However, as previously cited in Section 1.4.1, it is found by even an exceedingly meticulous experimentalist that, in earth gravity, the counterflow diffusion flame becomes highly unstable, and the planar symmetry is lost, for $a \leq 5 \text{ sec}^{-1}$, i.e., for flow-residence time of $(1/a) \approx 0.2 \text{ sec}$ (Sanchez *et al.* 1995). For most counterflow testing, the instability is observed for $a \leq 20 \text{ sec}^{-1}$. *While a nearly strain-rate-free planar diffusion flame is inaccessible in earth gravity for diagnostic probing, we believe that a planar diffusion flame is accessible in microgravity. Because (with all other parameters held fixed) the nearly strain-rate-free diffusion flame is the most vigorous and intense scenario for burning of initially segregated reactants, this limiting case is of appreciable pure and applied interest.* For example, consider the fundamentally and practically important scenario of hydrogen combusting with air, with the reactants initially separated and initially at room conditions. A reasonable estimate for the value of the frequency factor, with account being taken for the Arrhenius factor (evaluated at flame conditions), is $(B_f)_{\text{eff}} = \mathcal{O}(2 \times 10^5 \text{ sec}^{-1})$. Thus, the Damköhler number $D_1 \approx 0.4 \times 10^3$ for a strain rate $a \approx 20 \text{ sec}^{-1}$. The decrement from the thin-flame temperature for a second-order, finite-rate (but rapid) reaction is $\mathcal{O}(D_1^{-1/3})$, according to singular-perturbation estimates. For most counterflow testing in the laboratory, the peak temperature probably falls below the thin-flame temperature by an amount on the order of 10%, owing to strain-rate (limited-residence-time) effects. Thus, by the just-stated Damköhler-number criterion, diffusionally limited combustion is not anticipated to occur except in the limit $a \rightarrow 0$.

Sooting is precluded for tests with hydrogen as the fuel vapor, an already-noted motivation for selecting this species in the early testing. Other previously cited reasons for choosing hydrogen are: (1) the detailed chemical kinetics of hydrogen oxidation is simpler than the detailed chemical kinetics of the oxidation of a hydrocarbon vapor; and (2) hydrogen introduces exceptionally large differential diffusion (Lewis-Semenov-number effect), an effect of interest in assessing the adequacy of Burke-Schumann-type modeling. On the other hand, in the absence of sooting, only the relatively modest band radiation associated with water vapor enters, and we have already pointed out that optical detection of the hydrogen/oxygen diffusion-flame position is relatively challenging. In any case, later testing is to entail a hydrocarbon vapor as the

fuel species, so that sooting is anticipated; then, the continuous-spectrum, black-body flame luminosity associated with the presence of carbonaceous particulate abets the detection of the diffusion-flame position. In the absence of organized convective transport, the near-flame residence time of soot particles on the fuel side of the strain-rate-free diffusion flame is long; we anticipate that, if any nascent soot particles are formed, those particles have an opportunity to grow to exceptionally large size. Thus, the strain-rate-free planar diffusion flame affords an excellent opportunity to study the rates of sooting phenomena in diffusion flames. More generally, study of the formation of inorganic condensed-phase product species from the introduction of gaseous precursors into the strain-rate-free planar fuel-vapor/gaseous-oxidizer diffusion flame is facilitated.

2.0 BACKGROUND

2.1 Description of the Scientific Field; Prior Research

Within the more general subject of exothermic burning of initially separated gaseous reactants, we are concerned specifically with the limit of very intense, vigorous combustion. In the mathematical idealization of this limit, reaction is confined to an indefinitely thin interface at which the initially separated reactant species first encounter one another and are converted instantaneously to product species, so that the fuel species and oxidizer nowhere coexist. In the immediate vicinity of the indefinitely thin interface, diffusional transport of heat and species dominates convective transport, and the limiting scenario is called a *diffusion flame*. In common with other idealizations frequently adopted in continuum theory (*e.g.*, the vortex sheet, the shock wave, the contact surface, *etc.*), in practice there is always finite structure: for the diffusion flame, there is at least some interpenetration of the fuel and oxidizer species, because the chemical-kinetic rates are not infinitely rapid relative to transport rates, and (often less significantly) because some reverse reaction (dissociation of hot product species) occurs. Nevertheless, a diffusion flame can be very closely approximated physically. In a diffusion flame, the key processes involve fluid dynamics, in particular, convective motion and diffusive transport. The properties of the chemical-kinetic rates enter more and more significantly for conditions under which the fluid-element residence time is not long relative to the characteristic time for chemical reaction. As the spatial domain over which significant chemical reaction occurs becomes more distributed, the fuel and oxidizer interpenetrate and coexist over a larger region, and the highest temperature attained in the reacting flow falls. The rate of species conversion and heat release decreases when not just the transport of fresh preheated reactant to

the flame, but also the rate of conversion of the reactant once it is transported to a region of high temperature, inhibit the rate of burning. Accordingly, we are here concerned foremost with the establishment of a diffusion flame in a closed container; however, as the population of the stoichiometrically deficient reactant is depleted by reaction, we expect to convert from a diffusion flame to a less intense mode of combustion of initially separated reactants, and ultimately to extinction. For the large-activation-temperature kinetics typical of exothermic chemical processes, there is exponential sensitivity to the decrement in temperature in the reaction zone, and the transition from intense burning to extinction can occur in a few seconds or less.

The transport, in the immediate vicinity of the diffusion flame, of heat, mass, and momentum in the direction normal to the flame is important. Whereas any fluxes in the directions parallel to the flame are continuous across the flame, abrupt changes occur at the flame in fluxes of reactants, products, and heat which are perpendicular to the flame. Thus, the fluxes perpendicular to the flame establish the rate of reactant consumption and heat generation at the flame. While the configuration of a diffusion flame may be convoluted in an unsteady flow field, the structure of the flame is so thin that, locally and instantaneously, the largest gradients occur in the direction perpendicular to a planar flame (Carrier *et al.* 1975). Thus, to facilitate inspection of phenomena at a typical diffusion flame, we seek to create and sustain a macroscopically planar diffusion flame, so that we may monitor its properties, including its decay and extinction.

Unsteady, one-dimensional theoretical studies of strain-rate-free, long-residence-time diffusion flames have appeared in the literature (Bush and Fendell 1974; Liñán and Crespo 1976; Dold and Clark 1986). These isobaric studies elucidate properties of diffusion flames, without suggestion of how experimental verification might be achieved. Recently, with the advent of longer-duration testing time in microgravity, the advantages of a strain-rate-free planar diffusion flame in a container, for the convenience of both unsteady one-dimensional analysis and diagnostic probing, have become experimentally accessible. We suggest tracking the position and temperature of a planar diffusion flame in time in a squat closed container. The container is subdivided initially into a half volume containing diluted fuel vapor and a half volume containing diluted oxidizer, with the diffusion flame created at the planar interface between the half volumes, at the time of test initiation. Nonessential processes, such as reactant gasification from an initially condensed phase and such as net convective transport, are eliminated (or at least

minimized) by experimental design; sooting and significant radiative heat transfer may be added in later tests, but also are nonessential for the proposed first investigations of unsteady diffusive-reactive phenomena in unpremixed combustibles. The spherical counterpart of the Cartesian geometry (explicitly, a sphere of diluted fuel vapor, surrounded by an annulus of diluted oxidizer, all confined within an impervious noncatalytic spherical container) would permit the diffusion flame conveniently to close on itself, whereas near-cold-wall, flame-quenching phenomena have to be considered for a planar diffusion flame in any realistic, nonadiabatic, finite-dimension Cartesian apparatus (Fendell *et al.* 1994; Fendell and Wu 1995,1996). Nevertheless, in a spherical geometry, curvature effects would complicate the analysis, because the convenient introduction of a density-weighted (Lagrangian) spatial coordinate, to substitute for the physical radial coordinate, does not "go through"; experimentally, the intrusion required to fill the "inner" spherical subvolume (enveloped by the "outer" annular subvolume) would be complicated at best and compromising of the intended phenomena at worst. The most plausible candidate for a readily removable spherical interface, to separate the contents of the two subvolumes prior to test initiation, is a soap bubble. However, a soap bubble is of uncertain stability, and leaves a vitiating residue when it is broken at test initiation. Hence the planar-flame geometry seems preferable.

The objective of the current research is, through experimental design, to measure key properties of a diffusion flame for a fuel/oxidizer system of interest (such as flame temperature and position for hydrogen/oxygen reactants), and then to ascertain what assignment of values to the transport properties (in particular, the Lewis-Semimov numbers) permit a simplistic tractable model to recover these features most accurately. Practical guidance concerning the numerical assignment of input parameters, to which key system behavior is sensitive, is thereby furnished, and hopefully this guidance will prove useful in a broad context.

2.2 Current Research and Its Applications

While exceptions can be cited (*e.g.*, Otto-cycle internal-combustion engines, innovative natural-gas-fired gas turbines to meet the ultra-low-NO_x emissions standards in special environmental situations, and small natural-gas-fired flames for cooking), the preponderance of combustor designs entails mixing-controlled burning, for reasons of safety against explosions, stability against pressure spikes and flame oscillations, and ease of control/programmability. Also, most scenarios involving unwanted fire involve mixing-limited burning between the vapor of an initially condensed-phase fuel and atmospheric oxygen. In elucidating properties of the

laminar diffusion flame, we are discussing the basic building block of most practically encountered turbulent flames.

Characterization of diffusion flames by Burke-Schumann-type models has been traditionally favored because the procedure: (1) involves a selfconsistent level of approximation of the contributing aerothermochemical phenomena; (2) requires specification of a minimal number of input parameters that are unknown or highly uncertain; (3) is relatively amenable to facile mathematical solution; (4) provides output concerning the basic energetics and major species -- information of particular practical value for estimation of performance, and results particularly amenable to experimental verification; and (5) furnishes a "framework solution" that then can be used either to estimate trace-level-species populations by perturbation, or to serve as an initial approximation for the numerical solution of more detailed, computationally demanding formulations. We now address in more detail the relationship of Burke-Schumann-type models to the more intricate formulations to which much contemporary research is directed.

Modeling in recent decades has incorporated multistep, detailed chemical kinetics and multicomponent diffusion in the formulation of flame-structure studies; such inclusion is enabled by the rapid evolution of high-speed, large-storage computational capacity. Next to such highly inclusive formulation, the Burke-Schumann formulation (and extensions thereof, to encompass differing diffusivities) might seem relatively simplistic and perhaps outmoded. In fact, however, another emphasis in recent years -- trying to infer very highly reduced chemical-kinetic models which can replicate the key features of detailed treatments (Smooke, M.D., ed. 1991; Peters, N., and Rogg, B., eds. 1993) -- indicates the continued contribution to be made by Burke-Schumann-type models, not just for didactic purposes, but also for guidance in practical design.

Extensive parametric investigation with highly detailed models of combustion typically is feasible with current computing capacity, and probably with the computing capacity anticipated indefinitely into the future, only for steady one-dimensional and two-dimensional scenarios, involving simplistic dynamics and radiative heat transfer. However, practical hardware, such as furnaces, boilers, combustion chambers for propulsion, *etc.*, involves unsteady three-dimensional flows, with varied significant phenomena occurring on such disparate spatial scales that the direct incorporation of highly inclusive treatment of flamelet-scale phenomena is not feasible. What is required is a means of incorporating the consequences of subgridscale flamelet phenomena in computation carried out on the relatively gross mesh appropriate for combustor scale. Computation of flame structures by detailed models does not seem feasible for use in such

practical-application contexts, without the storage of tabulated results for flame structure. The formidable amount of tabulated computation could be rendered moot or obsolete in the face of continually updated information concerning rates, mechanisms, and transport coefficients.

Undertaking more detail in modeling offers an opportunity for the introduction of error as well as fact. Given a capacity to estimate the temporal and spatial distribution of the "flame-surface area per volume of space", the relatively simplistic Burke-Schumann formulation, or modest generalizations thereof, remains a feasible means of incorporating information about flamelets in computer models of mixing-controlled-combustion hardware (Carrier *et al.* 1974). The Burke-Schumann formulation is amenable to rapid solution as needed, or re-solution as upgraded information of input-parameter values becomes available. We reiterate that the Burke-Schumann solution holds for conditions of vigorous burning, and thus provides insight concerning a well-defined, high-performance limit. Typically, this information provides particularly useful guidance for design and upgrade.

2.3 The Proposed Experiment

2.3.1 Diffusion-Flame Initiation: Fluid-Dynamical Considerations

The obvious prerequisite to the monitoring of the properties of a planar diffusion flame (e.g., its temperature and position during its travel and burnout under microgravity, within a squat rectangular container with noncatalytic, impervious, isothermal walls) is creating such a planar flame in the first place. As noted in Section 1.1.3, the primary experimental demonstration for the Science Concept Review is the achievement of a planar diffusion flame at the near- z -coordinate-centerplane interface between the nonhypergolic fuel (argon-diluted hydrogen) and oxidizer (helium-diluted oxygen).

We seek the rapid withdrawal of an impervious thin flat separator by translation in its own plane, at a constant speed in a fixed direction, in order to create a planar discontinuity in composition between two masses of gas at the same initial temperature and pressure. For ideal (inviscid) fluids, the separator could be removed through a tightly sealed, near-centerplane slit in a side wall of the container, so that the rapid withdrawal induces no motion in the two masses of gas. In fact, the withdrawing separator cannot instantaneously achieve and maintain constant speed. More significantly, all conventional fluids have finite viscosity; there is no slip of the gases at the separator relative to the withdrawing separator, and continuity of stress implies that further gas is entrained into a wake flow aft of the trailing edge of the withdrawing separator.

The upshot is that a recirculatory flow is induced by the motion of the separator, wherein fluid in each half volume is transported, in a relatively thin near-centerplane shear layer, toward the side wall through which the separator is withdrawn, and this motion persists for a while even after the trailing edge of the separator has exited the chamber through the tight seal. By continuity, as some fluid is "dragged" across the chamber, other fluid moves toward the centerplane to occupy the volume formerly filled by the transported fluid. Within each half volume, the fluid transported to the side wall, but not permitted to exit because the seal around the withdrawing plate is tight, then necessarily turns toward the end wall in its half volume, and thereafter flows back in the direction from whence it came. The return drift is relatively broad and flow, in comparison with the rapid, oppositely directed flow in the narrow layer near the centerplane. Nothing precludes some of the entrained fluid from forming counterrotating vortices in the upper half and low half volume, near the side wall through which the separator is withdrawn (Tabaczynski *et al.* 1970); viscous dissipation eventually eliminates these local features. The upshot is that an organized convection, somewhat reminiscent of a counterflow, enhances diffusional transport toward the centerplane at early times, but this motion can be estimated. The motion effectively ceases at a time $t \approx 6W/u_o$, where u_o is the average speed of separator translation, $2W$ is the length of a side of the square cross section, and $t = 0$ is the time of the initiation of withdrawal. For $2W = 25 \text{ cm}$ and $u_o = 100 \text{ cm/sec}$, this motion is effectively over in about a second or so. More precise estimation is difficult because neither a meticulous numerical solution nor an instrumented experimental investigation of this withdrawing-shutter problem seems to have been reported. We estimate that flat-plate-withdrawal speeds u_o much in excess of 3 m/sec, maintained over 25 cm, may well cause transition from laminar to turbulent flow, if not in the Rayleigh-type boundary layers on each face of the withdrawing separator, then in the wake behind the trailing edge; such transition would enhance the entrainment and result in a more disruptive recirculatory flow (Sato and Kuriki 1961). Also, too rapid a withdrawal of a thin broad sheet might cause the undesirable onset of flutter, and, after onset, put more energy into the nonplanar, flutter-related motion. On the other hand, the total amount of fluid entrained during separator withdrawal under laminar flow varies as $u_o^{-1/2}$, so too slow a withdrawal speed is also problematic. Furthermore, the longer the interval for withdrawal, the longer the time span before events near the side wall through which the separator is withdrawn can replicate the events that occurred earlier near the facing side wall. Since we seek to achieve a cross-sectionally uniform, one-dimensional experiment, the slower the withdrawal, the more the

intended planarity of the subsequent fluid behavior is compromised. Indeed, we now discuss still other considerations that must be reconciled in the choice of the "average" separator-withdrawal speed u_o .

2.3.2 Diffusion-Flame Initiation: Mixing and Flame-Propagation Considerations

The withdrawal of the separator permits the interdiffusion of the reactants. A layer with (z -coordinate) thickness proportional to $2\{D[t - t_1(x)]\}^{1/2}$ forms near the centerplane, where D is an effective diffusion coefficient for hydrogen/oxygen at ambient conditions, t is time (with $t = 0$ recalled to be the start of separator withdrawal), and $t_1(x)$ is the time at which the trailing edge of the separator clears station x , where $x = 0$ is the plane of the side wall from which the separator is withdrawn [so $t_1(x) = x/u_o$]. The layer of interpenetration plausibly must be roughly on the order of several millimeters in thickness, δ , for the layer of interpenetrated reactants to be able to sustain a flame propagation against heat losses, since a distance of several millimeters is roughly the thickness of a propagating laminar flame at ambient conditions. Thus, $x_p(t) = u_o t$ gives the position of the trailing edge of the separator over the time span $0 \lesssim t \lesssim (2W/u_o)$; $x_e(t) \approx u_o t/3$ gives the position of the trailing edge of the domain with "significant" wake flow; and $x_c(t) = u_o [t - \delta^2/(4D)]$ gives the position (in general, within the wake) at which a combustible layer has formed behind the withdrawing separator; typically, $x_e(t) < x_c(t) < x_p(t)$.

Ignition, near the centerplane and near the side wall from which the separator is withdrawn, and after a time $\delta^2/(4D)$ has elapsed to ensure the formation of a combustible mixture, initiates a flame propagation through the stratified mixture in the vicinity of the centerplane. We take the site of ignition not to be so close to the side wall that the flame kernel decays because of heat loss to the cold wall; rather, the flame is taken to propagate at speed v_f across the expanse of the square cross-section. Because the combustible mixture is stratified, from the fuel-lean flammability limit on the "oxidizer side" of the centerplane to the fuel-rich flammability limit on the "fuel side" of the centerplane, no one speed really characterizes the rate of flame propagation; in fact, the speed v_f may be taken to be the maximum speed of propagation, probably holding for a near-stoichiometric mixture. (The peak flame speed holds for somewhat fuel-rich stoichiometries for a hydrogen/air mixture; corresponding data for our case of stratified hydrogen/argon-oxygen/helium are not available.) By definition, the speed of flame propagation goes to zero at sites with mixture at the fuel-lean or fuel-rich flammability

limit. Thus, a nonplanar flame front propagates in the x direction across the expanse of the square cross-section; the flame front has the configuration, in the z direction, of a crescent, with the extremes of the crescent not extending far above or far below the centerplane $z = 0$ (unless, for some reason, we delay the above-discussed ignition, and permit more interpenetration prior to arrival of the propagating flame). The crescent has curvature such that the flame front is most advanced in x near $z = 0$, and most retarded in x at its tips. The propagating flame is also quenched in the immediate vicinity of the cold side walls $y = 0$ and $y = 2W$, but this is a minor detail. The interpenetrated, stratified reactants at a given position x are converted to product species to the extent permitted by stoichiometric considerations; thus, the conversion of reactants is expected to be relatively complete at those strata (in the interpenetration layer) at which the fuel and oxidizer coexist in nearly stoichiometric proportions prior to reaction. However, as we look further and further toward the increasingly fuel-rich side of those strata, there is more and more "excess" fuel remaining after the flame propagation; analogously, as we look further and further toward the increasingly fuel-lean side of those strata, there is more and more "excess" oxidizer remaining after the flame propagation. At strata at which greater exothermic conversion of reactant species to product species occurs, we anticipate higher temperature. The combustion continues aft of the crescent-configured propagating flame in the form of a planar diffusion flame, where the plane of the flame is $z \approx 0$ at "early" time. In earth gravity, Rayleigh instability quickly disrupts the planarity of the diffusion flame, but the diffusion flame remains planar in microgravity. Such a crescent-shaped-premixed-flame/short-lived-planar-diffusion-flame configuration has been often observed in the aftermath of a localized ignition in an inhomogeneous fuel/oxidizer mixture with planar strata oriented perpendicular to the direction of earth gravity. For example, a relatively light fuel vapor such as methane collects near the ceiling of a mine gallery, air collects near the floor, and strata with intermediate composition lie between. The trident-shaped flame configuration is referred to as a triple flame or three-branched flame. The triple-flame phenomenology may well warrant investigation for both its inherent fundamental interest and its possible practical importance (*e.g.*, besides mine safety, the triple flame may play an important role in the stabilization of those turbulent jet diffusion flames which are observed to be lifted from the lip of the fuel-vapor-issuing nozzle). Indeed, the present apparatus seems particularly suitable for the experimental investigation of triple-flame phenomenology, which (as just noted) is a commonly occurring mechanism in the spatial evolution of diffusion flames from cold, nonhypergolic, initially separated fuel vapor and oxidizer. However, attention here is focused on the subsequent behavior of the planar diffusion

flame engendered via the triple flame, not on the triple flame itself. In order to ensure the one-dimensionality of the subsequent travel of the diffusion flame, we seek as rapid a triple-flame propagation across the centerplane as is permitted by physical constraints (*e.g.*, avoiding transition to turbulence) and experimental procedure (*e.g.*, limitations of pull mechanisms for separator withdrawal, in view of size, weight, reliability, and cost constraints for microgravity testing).

2.3.3 Diffusion-Flame Initiation: Spark Siting and Timing

We have discussed the near-centerplane flame propagation in the x direction as if a line ignition near the side wall $x = 0$ were feasible -- we have accounted for no dependence on the y coordinate, other than the near-cold-wall quenching at $y = 0$ and $y = 2W$. In fact, about ten, evenly spaced pairs of electrodes are to be used to generate simultaneous sparks and flame kernels near one side wall at $z \approx 0$. The flame fronts evolving from each pair of the ten-or-so, linearly arranged electrodes propagate through the mixture, and neighboring flame fronts merge in time. Since the mixture can undergo exothermic conversion from reactant species to product species but once, the intersection of flames from neighboring electrodes results in a single "corrugated" front. In time, the corrugated configuration of the merged flame fronts evolves into a flame front with greater uniformity in the y coordinate. Clearly, since the distance in the x direction that the flame must propagate to achieve a given uniformity in the y coordinate decreases with more spark-ignition sites, it is experimental considerations that limit the number of electrode pairs to about ten.

We seek to minimize the temporal interval (after initiation of separator withdrawal at time $t = 0$) for the creation of a diffusion flame spanning virtually the entire expanse ($0 \bar{z} y \bar{z} 2W$, $0 \bar{z} x \bar{z} 2W$, where $2W = 25 \text{ cm}$) of the plane $z \approx 0$, so that the subsequent phenomena may be taken as one-dimensional in the core of the container, to good approximation. The choice of spark timing is set by this consideration. The longer that spark ignition is delayed after time $t = 0$, the longer the flame must propagate at a speed limited to the value v_f or smaller. A plausible value for the flame-spread speed v_f for a near-stoichiometric mixture formed from the mixing of highly fuel-lean hydrogen/argon with highly oxidizer-rich oxygen/helium is about 50 cm/sec. [A highly fuel-lean hydrogen/argon mixture is adopted so that the peak diffusion-flame temperature will be moderate ($\sim 2000 \text{ K}$ or less), and the expansivity of the burned gas will not be so large that all the unburned hydrogen becomes

confined to a very thin layer contiguous to the end wall at $z = -L$.] We ignite at time $t = t_{ig} (> 0)$, a finite interval after initiation of withdrawal of the separator; we ignite near $x = 0$, *i.e.*, in the proximity of the side wall from which the trailing edge of the separator departs at time $t = 0$. We note that the trailing edge of the withdrawing separator is at position $x_p(t) = u_o t$; the trailing "edge" of the wake flow is at position $x_e(t) \approx u_o t/3$, and the most advanced position of the propagating flame is at position $x_f(t) = v_f(t - t_{ig})$. We recall that $t_{ig} > [\delta^2/(4D)]$ lest the spark be dissipated in gas that cannot sustain a flame propagation. We investigate the consequences of delaying the sparking longer than this minimal interval (probably in excess of 4 msec). Actually, the expansion of already burned gas might result in a displacement of the position of the propagating flame further across the centerplane than the position given by the above formula for $x_f(t)$, so the adopted expression for $x_f(t)$ is "conservative"; however, except for very briefly after ignition, we expect most of the expansion consequent on the burning to result in displacement of the burned-gas-occupied domain toward $z = \pm L$, not toward larger values of x -- owing to the thin-layer geometry of the burned gas. Thus, we retain the above expression for $x_f(t)$ for the purposes of estimation. If the propagating flame catches up with the trailing edge of the wake flow, thenceforth the position of the flame advances with a speed that is the *sum* of the convective transport speed in the wake flow *plus* the flame-propagation speed; thus, very shortly after the propagating flame catches up with the trailing edge of the wake flow, the flame propagates as close to the trailing edge of the withdrawing separator as the distance required for the formation of a combustible mixture (and the quench layer near the cold separator surface) permits. (There is no physical mechanism by which combustion can exist at, or in front of, the trailing edge of the withdrawing separator plate, under the anticipations described here.) The time $t = t_{cu}$ at which the flame propagation catches up with the trailing edge of the wake is given by equating the expressions for $x_f(t)$ and $x_e(t)$:

$$t_{cu} = \frac{v_f t_{ig}}{v_f - (u_o/3)}, \quad (2.1)$$

where catch-up occurs only if $v_f > (u_o/3)$, and t_{cu} must be somewhat less than $(2W/u_o)$ if catching up with the wake is to result in (virtually) catching up with the trailing edge of the withdrawing plate. For $v_f = 50$ cm/sec and $u_o = 75$ cm/sec, t_{ig} must be somewhat less than (1/3) sec for the flame to spread across the centerplane as rapidly as it can (*i.e.*, almost as rapidly

as the trailing edge of the withdrawing separator departs the test chamber), for the given parametric assignments.

3.0 JUSTIFICATION FOR CONDUCTING THE EXPERIMENT IN SPACE

3.1 Limitations of Ground-Based Testing

In Section 1.4, we presented the major considerations that preclude meaningful execution of the proposed experiment in ground-based microgravity facilities. The slow travel of a planar diffusion flame in a closed container of the dimensions specified in Section 1.4.1 requires a testing interval appreciably greater than that (~ 2 - 5 sec) available in drop towers. Furthermore, the choice of suitably large dimensions for the container, so that the gas-phase phenomenon in the core of the container is not corrupted over the testing time span (~ 10 - 30 sec) by wall-induced deviations, is contingent on uniformly maintaining a gravitational acceleration of $10^{-5} g_0$, where g_0 is recalled to be the magnitude of the earth gravity. This constraint precludes testing in aircraft.

Here we append several comments for which we did not wish to interrupt the narrative in Section 1.4. First, we address whether instabilities arising early, during diffusion-flame initiation, may be more disruptive than instabilities arising later in the test. For example, at very early time, the diffusion flame is generated near the centerplane, but very little heat has reached the upper planar end wall $z = +L$, so the appropriate vertical scale for use [in assessing whether the critical Rayleigh number (defined in Section 1.4.1) for the growth of instabilities is exceeded] is a distance less than L . However, if we envision the start-up scenario in the quasi-steady approximation, so that the length appropriate for substitution in the critical Rayleigh number takes on a succession of increasing values, then the most challenging condition for maintaining stability is the one examined previously, the one in which the half-chamber height L is the appropriate assignment for the length. Thus, the challenge to maintaining planarity is smaller, not greater, during the start-up scenario.

Owing to changes during flight in orientation of the gravitational force, such that the force does not act entirely perpendicular to the end walls at $z = \pm L$, or owing to transverse temperature gradients arising during diffusion-flame initiation and/or in connection with cold-side-wall-induced flame-quenching thermal boundary layers, density differences perpendicular to the gravitational acceleration may arise. The critical Rayleigh number for "sidewise" temperature gradients is zero; *i.e.*, fluid motion immediately ensues as a consequence of the

existence of any finite temperature gradient *perpendicular* to a component of the gravitational acceleration. For the minimization of this buoyancy-induced transverse velocity, we seek as small as possible a magnitude of the gravitational body force throughout the testing interval. This consideration again suggests the desirability of a gravitational acceleration of $10^{-5} g_0$.

3.2 Limitations of Mathematical Modeling

3.2.1 Empirical Assignment of the Lewis-Semenov Numbers in Multicomponent Gases

The adoption of the Burke-Schumann limit in the mathematical modeling of diffusion flames approximates the finite rate of chemical reactions in initially separated reactants to be indefinitely rapid, relative to transport rates. Chemical conversion of reactants to products is confined entirely to mathematically thin interface(s) in space, as a suitable approximation to the narrow but finite structure of such flames. Adoption of the Burke-Schumann limit obviates the physical and mathematical challenges of furnishing chemical-kinetic rates and mechanisms, and isolates the challenge that remains -- the modeling of the transport coefficients for heat and species in multicomponent gases of changing composition. The thermal conductivity and species diffusion coefficients in a Burke-Schumann model are adopted in the forms derived for a binary mixture; the adequacy of binary-diffusion forms for use in the description of transport phenomena in multicomponent media has not been extensively investigated experimentally. As pointed out by Zeldovich *et al.* (1985), the binary-mixture approximation for a multicomponent mixture *seems* appropriate for the commonly encountered case of combustion of a hydrocarbon fuel with air. For the complete oxidation of the hydrocarbon species C_nH_m with air under fuel-lean or stoichiometric conditions, one mole of the fuel burns with approximately $4.77 [n + (m/4)]$ moles of air, of which about $3.77 [n + (m/4)]$ moles are N_2 . While there is some trace-level dissociation of N_2 at high combustion temperature, sometimes with significant environmental impact, mostly the diatomic nitrogen remains intact. Thus, in typical combustion, both the reactants and products exist mostly in a "sea" of nitrogen, and the binary-mixture coefficients are inferred to suffice. Even in the combustion of initially separated reactants, this statement holds because (in view of cost, availability, toxicity, and pollution considerations) the most commonly used diluent for (say) a natural-gas-feed line is N_2 .

In the planar-diffusion-flame experiment, we have devised initial conditions in a closed container so that the thermodynamic state of the contents of each of two half volumes is uniform, and so that the average molecular weight of the contents of the two half volumes are identical.

We expect that the initial conditions have been so contrived that, throughout the test interval, the average molecular weight remains roughly constant. Accordingly, the statement of the equation of state for the multicomponent mixtures is well approximated by the equation of state for a one-component mixture at that average molecular weight. Furthermore, the binary-collision model for the species-diffusion coefficients ought to be appropriate, since any species, on average, is colliding with a particle with roughly the average molecular weight of all the contents of the container. In short, for our first test cases, we have identified conditions particularly suitable for data interpretation by the application of the Burke-Schumann model, without incurring the complication of either carbon or nitrogen chemistry; we do not rely on a "sea" of nitrogen to justify the adoption of a binary-diffusion treatment of species transport. Nevertheless, even upon granting that our first test cases are well chosen to achieve this end, limitations on the mathematical modeling remain, as we now develop.

In the experiment on a planar diffusion flame in microgravity, we seek to identify what assignments for the Lewis-Semenov numbers suffice for accurate diffusion-flame description, within the Burke-Schumann framework. [The Lewis-Semenov numbers $(Le)_j$ are recalled to the ratios of the Fickian diffusion coefficient for species j , D_j , to the thermal diffusivity for the mixture, κ . Actually, the definition $(Le)_j \equiv D_j/\kappa$ is the inverse of the conventional definition, but is convenient here. The Burke-Schumann model takes both D_j and κ to vary in value similarly with the local thermodynamic state, so that the ratio $(Le)_j$ is invariant in both space and time; the designation $(Le)_j$ indicates that, in general, a different (constant) value holds for each species j .]

In the most simplistic version of the Burke-Schumann framework, the assignment $(Le)_j = Le$, independently of j , is adopted for all species j , typically with $Le = 1$; under the global (overall), one-step mechanism adopted within the Burke-Schumann framework, with boundary and initial constraints permitting, adoption of unity for the Lewis-Semenov numbers implies a linear relationship between: (1) sensible heat, and (2) chemical heat, in the form of mass fractions of either reactant species, the exothermicity from which has yet to be released, or product species, whose presence (in cases of interest here) is indicative of already-released exothermicity. [Of course, $(Le)_j = Le$ implies $D_j = D$, so that linear relationships also hold between the mass fractions of the fuel species and of the oxidizer species, between the mass fractions of the fuel species and of the product species, and between the mass fractions of the

oxidizer species and the product species.] In any specific scenario, identifying the explicit expressions for the linear relationships between the just-enumerated combinations of the dependent variables requires solving no more than convective-diffusive balances over a known, well-defined domain. In short, the mathematical statement of the diffusion-flame problem is formally reduced to the mathematical statement of the distribution of a chemically inert species. Thus, we forego much simplification if we abandon the mathematically convenient approximation that $(Le)_j = 1$; nevertheless, we must do so on physical grounds for the first case to be examined here, because hydrogen and oxygen do not diffuse at comparable rates. We tentatively retain the expectation that the factors $(Le)_j$ can be satisfactorily approximated as constants. The first step in ascertaining appropriate values for $(Le)_j$ is solving the convective-diffusive balances. However, now a convective-diffusive balance holds for an individual variable, such as the fuel mass fraction, the oxidizer mass fraction, and the temperature, and the balance holds over a domain, part of whose boundary is the (translating) position of the flame and hence ascertained only in the course of solution. The results of the Stefan problem are to be compared with observation, to establish what values of the Lewis-Semenov numbers $(Le)_j$ permit the solution to fit the observations of flame position and temperature.

The above-mentioned limitation to a Burke-Schumann-type aerothermochemical model is now discussed. If ρ_j denotes the density of gaseous species j , and \vec{v} , the velocity, then conservation of species j requires

$$\frac{\partial \rho_j}{\partial t} + \nabla \cdot [(\rho_j \vec{v}) + (\rho Y_j \vec{V}_j)] = w_j, \quad (3.1)$$

where: t denotes time; the mass fraction of species j , $Y_j = \rho_j / \rho$; w_j is the rate of production of species j ; and \vec{V}_j is the diffusion velocity of species j . Fick's law suggests, with D_j denoting the mass-transfer coefficient of species j ,

$$\frac{\partial \rho_j}{\partial t} + \nabla \cdot (\rho_j \vec{v}) - \nabla \cdot (\rho D_j \nabla Y_j) = w_j. \quad (3.2)$$

Upon summing over all species, $j = 1$ to $j = N$, since $\sum_{j=1}^N \rho_j = \rho$,

$$\frac{\partial \rho}{\partial t} + \nabla \cdot (\rho \bar{v}) = 0, \sum_{j=1}^N w_j = 0, \quad (3.3a, 3.3b)$$

where Equation (3.3a) is identified as the (global) continuity equation and Equation (3.3b) states that no net mass is created or destroyed via chemical reaction. Hence,

$$\nabla \cdot \left(\rho \sum_{j=1}^N D_j \nabla Y_j \right) = 0. \quad (3.4)$$

For $D_j \equiv D$, independently of j , we have $\sum_{j=1}^N Y_j = 1$, and Equation (3.4) is reduced to an identity. More generally, we see that Fickian diffusion with $(Le)_j$ equal to a constant dependent on j only, cannot hold for all species present (Williams 1985). We elect to adopt Fickian diffusion for species $j = 1, 2, \dots, N-1$, and to identify

$$Y_N = 1 - \sum_{j=1}^{N-1} Y_j, \quad (3.5)$$

where we select Y_N to be the product species.

Thus, the adequacy of the inevitably approximate models that are introduced to achieve mathematical tractability within the physical constraints requires experimental evaluation. The intention here is to use a subset of the data to assign values to the Lewis-Semenov numbers $(Le)_j$, so that solution of a generalized Burke-Schumann model can recover key features of the experimental observations. The universality of these assignments of values to the Lewis-Semenov numbers is to be evaluated by seeing how well the key observed features of the rest of the data can be recovered. Of course, this is to be an iterative process until optimal assignments of the Lewis-Semenov numbers are identified. Finally, an assessment of the viability of this generalized Burke-Schumann model for prediction of diffusion-flame behavior is to be undertaken. Whether or not a generalized Burke-Schumann model proves sufficiently robust, the experiment will furnish a unique, novel, fundamental data set for the testing of any diffusion-flame model.

3.2.2 Estimation of the Time to Diffusion-Flame Extinction

As noted in Section 1.5, in the Burke-Schumann model, the first Damköhler number D_1 , the ratio of a characteristic time for transport to a characteristic time for chemical reaction, is taken as indefinitely large. According to this idealization, extinction of chemical reaction occurs only when the initial amount of fuel (for the fuel-deficient scenarios of interest here) is totally depleted, as signified by the travel of the diffusion flame to the end wall ($z = -L$, by convention) of the fuel-containing half volume (Section 1.1.2). In fact, as the total amount of fuel becomes depleted, the characteristic time for chemical reaction to occur between fuel and oxidizer near the flame front increases; the law of mass action is a phenomenological quantification of the fact that fewer collisions of the oxidizing species occur with the residual reservoir of fuel species. Contrary to the Burke-Schumann model, extinction of chemical reaction occurs prior to the total depletion of the fuel presence. Quantifying the amount of residual fuel at extinction requires commitment to an expression for the rate of reaction between fuel species and oxidizer species at the local temperature and pressure. The simplest model is to adopt a direct one-step second-order irreversible reaction, with Arrhenius-type dependence on the local temperature. For the typical scenario, in which the value of the Arrhenius activation temperature is large relative to the thin-flame temperature, it is known (Fendell 1965) that, for quasisteady scenarios, there is a finite value of the first Damköhler number D_1 above which combustion must proceed vigorously; $D_1 > (D_1)_{ig}$ is a sufficient condition for intense burning. There is also a finite (smaller) value of the first Damköhler number, henceforth denoted $(D_1)_{ex}$, such that $D_1 < (D_1)_{ex}$ is a sufficient condition for extinction of chemical reaction. If the local characterization of the Damköhler number D_1 lies in the range $(D_1)_{ig} > D_1 > (D_1)_{ex}$, the burning may or may not be extinguished -- in this range, the alternatives of effectively extinguished or fairly strong burning may occur, and which is observed depends on prior history and disturbances. Thus, $D_1 > (D_1)_{ex}$ is a necessary condition for ignition, and $D_1 < (D_1)_{ig}$ is a necessary condition for extinction.

Interest here centers on the question of extinction of combustion after an interval of vigorous burning during a test, because of fuel depletion (and proximity of the flame to a cold wall, so there is appreciable heat loss). The sufficient criterion $D_1 < (D_1)_{ex}$ for extinction has been numerically tabulated for a direct one-step second-order irreversible Arrhenius-type

chemical reaction with Lewis-Semenov numbers unity, and then functionally curve-fitted for convenience in application (Liñán 1974); generalization to the case of constant, nonunity values of the Lewis-Semenov numbers is straightforward (*e.g.*, Fendell and Wu 1995). Properties of the Burke-Schumann, flame-without-structure solution must be available for checking whether the extinction criterion is met. It may seem paradoxical that the thin-flame solution must be in hand, in order to establish whether the thin-flame solution does not hold according to a finite-reaction-rate model. However, the sufficient criterion for extinction is based on a singular-perturbational analysis in which "corrections" to the thin-flame solution arise only in the immediate vicinity of the thin flame, to account for nascent interpenetration of reactants; aside from this local but crucial modification, the dependent-variable profiles of the Burke-Schumann solution remain excellent lowest-order approximations to the solution with full account taken of the effect of the finite-rate chemistry (Zeldovich 1945). In fact, it is this very localization of the consequences of the role of finite-rate kinetics, even at extinction, that permits derivation of a flame-geometry-independent, universally applicable criterion for diffusion-flame extinction under a one-step model.

The Burke-Schumann estimate of the time to extinction of the burning is an upper bound because it relies on total depletion of the deficient reactant. The accuracy of the typically small correction afforded by the just-described sufficient condition for extinction depends on how well the assignment of values to parameters of the one-step chemical-kinetic model incorporates the actual detailed chemical rates and mechanisms. It is possible to bypass the entire large-but-finite-Damköhler-number-based extinction modeling and, instead, to adopt (say) a flame temperature below which the thin-flame model no longer plausibly holds. For the large-activation-temperature chemical kinetics characteristic of fuel/oxidizer pairs of practical interest for combustion, there is abrupt transition from highly vigorous combustion to effectively extinguished reaction; thus, virtually all residual fuel at the extinction condition should persist indefinitely.

4.0 REFERENCES

- Baumstein, A., and Fendell, F. (1998). Strain-rate-free diffusion flames: initiation, properties, and quenching. *Combustion Science and Technology* **132**, 157-198.
- Burke, S. P., and Schumann, T. E. W. (1928). Diffusion flames. *Industrial and Engineering Chemistry* **20**, 998-1004.

- Bush, W. and Fendell, F. (1970). Asymptotic analysis of laminar flame propagation for general Lewis numbers. *Combustion Science and Technology* **1**, 421-428.
- Bush, W. B., and Fendell, F. E. (1974). Diffusion-flame structure for a two-step chain reaction. *Journal of Fluid Mechanics* **64**, 701-724.
- Carrier, G. F., Fendell, F. E. and Bush, W. B. (1978). Stoichiometry and flame-holder effects on a one-dimensional flame. *Combustion Science and Technology* **18**, 33-46.
- Carrier, G. F., Fendell, F. E., and Marble, F. E. (1974). The effect of strain rate on diffusion flames. *SIAM Journal on Applied Mathematics* **28**, 463-500.
- Carslaw, H. S., and Jaeger, J. C. (1959). *Conduction of Heat in Solids*, 2nd ed. Oxford, England: Clarendon.
- Committee on Microgravity Research, Space Studies Board (1995). *Microgravity Research Opportunities for the 1990s*. Washington, DC: National Research Council.
- Crank, J. (1975). *The Mathematics of Diffusion*, 2nd ed. Oxford, England: Clarendon.
- Crank, J. (1984). *Free and Moving Boundary Problems*. Oxford, England: Clarendon.
- Dold, J. W., and Clark, J. F. (1986). Combustion of a finite quantity of gas released in the atmosphere. *Twenty-first Symposium (International) on Combustion*, pp. 1349-1356. Pittsburgh, PA: Combustion Institute.
- Fendell, F. (1965). Ignition and extinction in combustion of initially unmixed reactants. *Journal of Fluid Mechanics* **21**, 281-303.
- Fendell, F. E., Bush, W. B., Mitchell, J. A., and Fink IV, S. F. (1994). Diffusion-flame burning of fuel-vapor pockets in air. *Combustion and Flame* **98**, 180-196.
- Fendell, F. E. and Mitchell, J. A. (1996). Feasibility of planar, unidirectional-flow diffusion flames in earth gravity. *Combustion Science and Technology*, **120**, 83-117.
- Fendell, F., and Wu, F. (1995). Unsteady planar diffusion flames: ignition, travel, burnout. *Combustion Science and Technology* **107**, 93-126.
- Fendell, F., and Wu, F. (1996). Diffusion-flame burning of fuel vapor pockets in air for general Lewis numbers. *Combustion Science and Technology* **105**, 1-14.

- Feng, C. C., Lam, S. H., and Glassman, I. (1975). Flame propagation through layered fuel-air mixtures. *Combustion Science and Technology* **10**, 59-71.
- Friedlander, S. K., and Keller, K. H. (1963). The structure of the zone of diffusion-controlled reaction. *Chemical Engineering Science* **18**, 365-375.
- Gaydon, A. G., and Wolfhard, H. G. (1979). *Flames -- Their Structure, Radiation and Temperature*, 4th ed. London, England: Chapman and Hall.
- Goldstein, R. J., and Volino, R. J. (1995). Onset and development of natural convection above a suddenly heated horizontal surface. *Journal of Heat Transfer* **117**, 808-821.
- Hill, J. M. (1987). *One-dimensional Stefan Problems: an Introduction*. Essex, England: Longman Scientific and Technical.
- Ishikawa, N. (1983a). A diffusion combustor and methane-air flame propagation in concentration gradient field. *Combustion Science and Technology* **30**, 185-203.
- Ishikawa, N. (1983b). Flame structure and propagation through an interface of layered gases. *Combustion Science and Technology* **31**, 109-117.
- Ishikawa, N. (1983c). Flame propagation in time-independent concentration gradient fields. *Combustion Science and Technology* **35**, 207-213.
- Leal, L. G. (1992). *Laminar Flow and Convective Transport Processes -- Scaling Principles and Asymptotic Analysis*. Boston, MA: Butterworth-Heinemann.
- Liebman, I., Corry, J., and Perlee, H. E. (1970). Flame propagation in layered methane-air systems. *Combustion Science and Technology* **1**, 257-267.
- Liñán, A. (1974). The asymptotic structure of counterflow diffusion flames for large activation energies. *Acta Astronautica* **1**, 1007-1039.
- Liñán, A., and Crespo, A. (1976). An asymptotic analysis of unsteady diffusion flames for large activation energies. *Combustion Science and Technology* **14**, 95-117.
- Microgravity Combustion Branch (1995). *Microgravity Combustion Science: 1995 Program Update*. Cleveland, OH: Lewis Research Center, National Aeronautics and Space Administration.
- Penner, S. S. (1957). *Chemistry Problems in Jet Propulsion*. New York, NY: Macmillan.

- Peters, N., and Rogg, B., eds. (1993). *Reduced Kinetic Mechanisms for Applications in Combustion Systems*. New York, NY: Springer-Verlag.
- Phillips, H. (1965). Flame in a buoyant methane layer. *Tenth Symposium (International) on Combustion*, pp. 1277-1283. Pittsburgh, PA: Combustion Institute.
- Sanchez, A. L., Liñán, A., Williams, F. A., and Ballakreshnan, G. (1995). Theory of structures of hydrogen-air diffusion flame. *Combustion Science and Technology* **110-111**, 277-301.
- Sato, H., and Kuriki, K. (1961). The mechanism of transition in the wake of a thin flat plate placed parallel to a uniform flow. *Journal of Fluid Mechanics* **11**, 321-352.
- Smooke, M. D., ed. (1991). *Reduced Kinetic Mechanisms and Asymptotic Approximations for Methane-Air Flames* (Lecture Notes in Physics, Vol. 384). New York, NY: Springer-Verlag.
- Tabaczynski, R. J., Hout, D. P., and Keck, J. C. (1970). High Reynolds number flow in a moving corner. *Journal of Fluid Mechanics* **42**, 249-255.
- Williams, F. A. (1985). *Combustion Theory*, 2nd ed. Menlo Park, CA: Benjamin/Cummings.
- Yih, C.-S. (1979). *Fluid Mechanics -- a Concise Introduction to the Theory*. Ann Arbor, MI: West River.
- Zeldovich, Y. B. (1951). On the theory of combustion of initially unmixed gases. NACA TM 1296.
- Zeldovich, Y. B., Barenblatt, G. I., Lebrovich, V. B., and Makhviladze, G. M. (1985). *The Mathematical Theory of Combustion and Explosions*, translated by D. H. McNeill. New York, NY: Consultants Bureau.

REPORT DOCUMENTATION PAGE			Form Approved OMB No. 0704-0188	
Public reporting burden for this collection of information is estimated to average 1 hour per response, including the time for reviewing instructions, searching existing data sources, gathering and maintaining the data needed, and completing and reviewing the collection of information. Send comments regarding this burden estimate or any other aspect of this collection of information, including suggestions for reducing this burden, to Washington Headquarters Services, Directorate for Information Operations and Reports, 1215 Jefferson Davis Highway, Suite 1204, Arlington, VA 22202-4302, and to the Office of Management and Budget, Paperwork Reduction Project (0704-0188), Washington, DC 20503.				
1. AGENCY USE ONLY (Leave blank)	2. REPORT DATE February 1999	3. REPORT TYPE AND DATES COVERED Final Contractor Report		
4. TITLE AND SUBTITLE Unsteady Diffusion Flames: Ignition, Travel, and Burnout (SUBCORE Project: Simplified Unsteady Burning of Contained Reactants)			5. FUNDING NUMBERS WU-963-15-0G-00 NAS3-27264	
6. AUTHOR(S) Francis Fendell and Harald Rungaldier				
7. PERFORMING ORGANIZATION NAME(S) AND ADDRESS(ES) Electro-Optics, Lasers and Research Center TRW Space and Electronics Group One Space Park Redondo Beach, California 90278			8. PERFORMING ORGANIZATION REPORT NUMBER E-11466	
9. SPONSORING/MONITORING AGENCY NAME(S) AND ADDRESS(ES) National Aeronautics and Space Administration Lewis Research Center Cleveland, Ohio 44135-3191			10. SPONSORING/MONITORING AGENCY REPORT NUMBER NASA CR-1999-208686	
11. SUPPLEMENTARY NOTES Project Scientist, Suleyman Gokoglu, NASA Lewis Research Center, organization code 6711, (216) 433-5499.				
12a. DISTRIBUTION/AVAILABILITY STATEMENT Unclassified - Unlimited Subject Categories: 23, 28, 31, and 34 This publication is available from the NASA Center for AeroSpace Information, (301) 621-0390.			12b. DISTRIBUTION CODE Distribution: Nonstandard	
13. ABSTRACT (Maximum 200 words) An experimental apparatus for the examination of a planar, virtually strain-rate-free diffusion flame in microgravity has been designed and fabricated. Such a diffusion flame is characterized by relatively large spatial scale and high symmetry (to facilitate probing), and by relatively long fluid-residence time (to facilitate investigation of rates associated with sooting phenomena). Within the squat rectangular apparatus, with impervious, noncatalytic isothermal walls of stainless steel, a thin metallic splitter plate subdivides the contents into half-volumes. One half-volume initially contains fuel vapor diluted with an inert gas, and the other, oxidizer diluted with another inert gas—so that the two domains have equal pressure, density, and temperature. As the separator is removed, by translation in its own plane, through a tightly fitting slit in one side wall, a line ignitor in the opposite side wall initiates a triple-flame propagation across the narrow layer of combustible mixture formed near midheight in the chamber. The planar diffusion flame so emplaced is quickly disrupted in earth gravity. In microgravity, the planar flame persists, and travels ultimately into the half-volume containing the stoichiometrically deficient reactant; the flame eventually becomes extinguished owing to reactant depletion and heat loss to the walls.				
14. SUBJECT TERMS Diffusion flame; Microgravity combustion; Stefan problem			15. NUMBER OF PAGES 63	
			16. PRICE CODE A04	
17. SECURITY CLASSIFICATION OF REPORT Unclassified	18. SECURITY CLASSIFICATION OF THIS PAGE Unclassified	19. SECURITY CLASSIFICATION OF ABSTRACT Unclassified	20. LIMITATION OF ABSTRACT	